Supplementary Information for
Multiscale land-atmospheric feedbacks intensify hot droughts over global river-basins

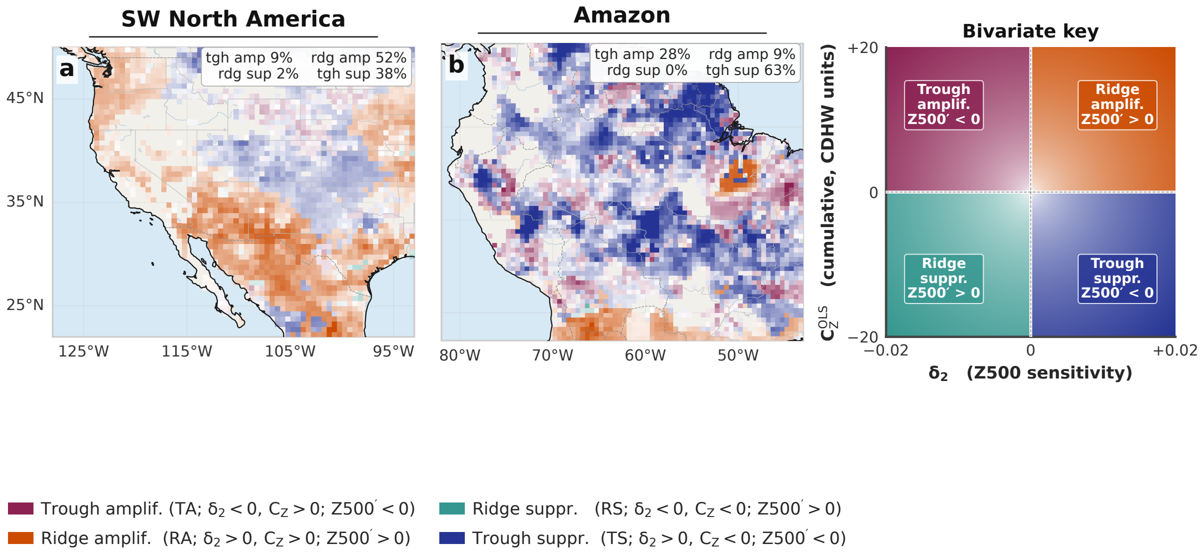

Supplementary Figure 1: Where and how strongly 500-mb geopotential height anomaly is associated with hot drought severity in south-western North America (a) and the Amazon (b).Each grid cell is coloured by two quantities simultaneously: δ_2 and $C_{Z_{500}}$.

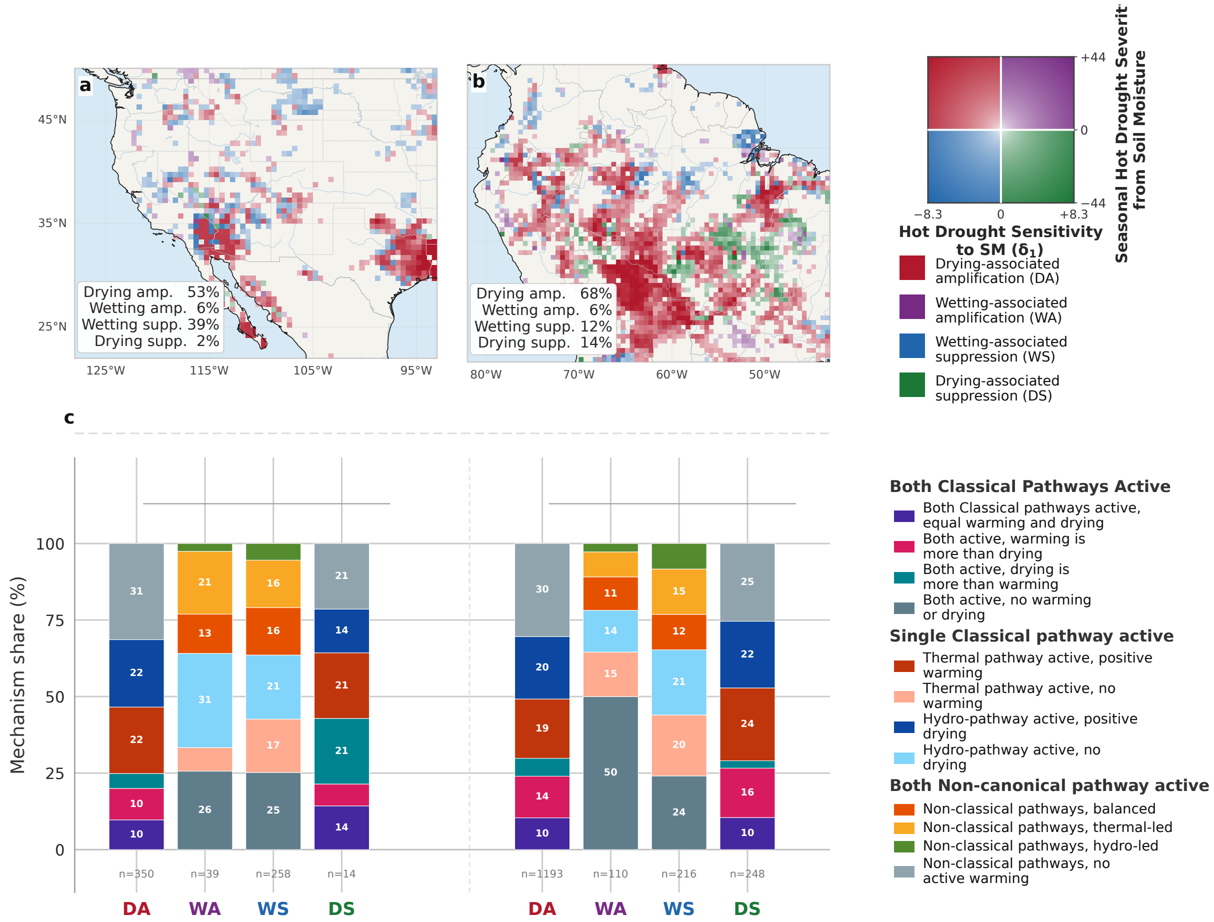

Supplementary Figure 2: Where and how strongly soil moisture is associated with hot drought severity in south-western North America (a) and the Amazon (b) in 2010 .Each grid cell is coloured by two quantities simultaneously: δ_1 and C_{SM}. Red (blue) tones indicate that dry (wet) soil is associated heat extremes. Color saturation reflects signal strength.(c,d) For each coupling regime identified in panels (a,b), the bars show what heterogenity in land-atmospheric feedback pathway of grid cells experienced.

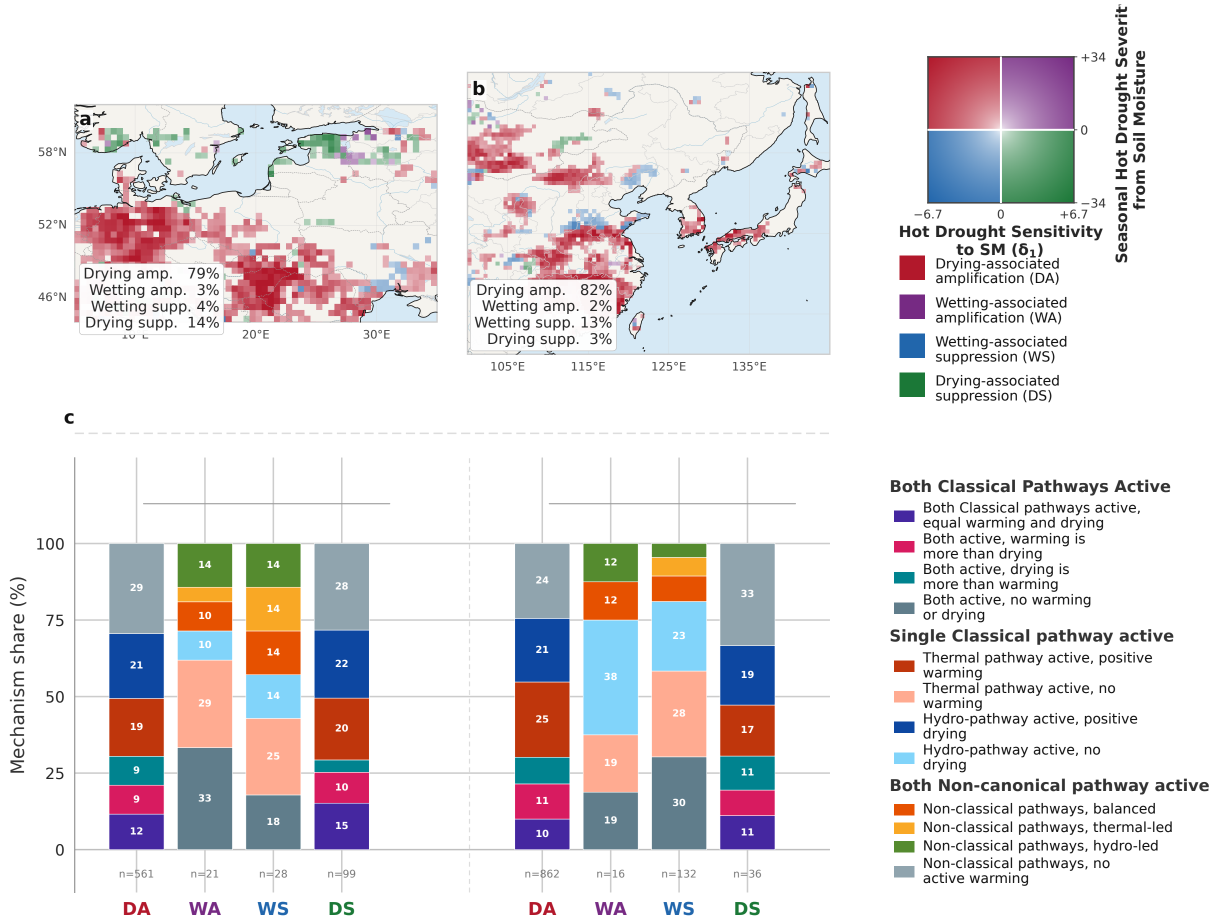

Supplementary Figure 3: Where and how strongly soil moisture is associated with hot drought severity in Central Europe (a) and (b) East in 2022 .Each grid cell is coloured by two quantities simultaneously: δ_1 and C_{SM}. Red (blue) tones indicate that dry (wet) soil is associated heat extremes. Color saturation reflects signal strength.(c,d) For each coupling regime identified in panels (a,b), the bars show what heterogenity in land-atmospheric feedback pathway of grid cells experienced.

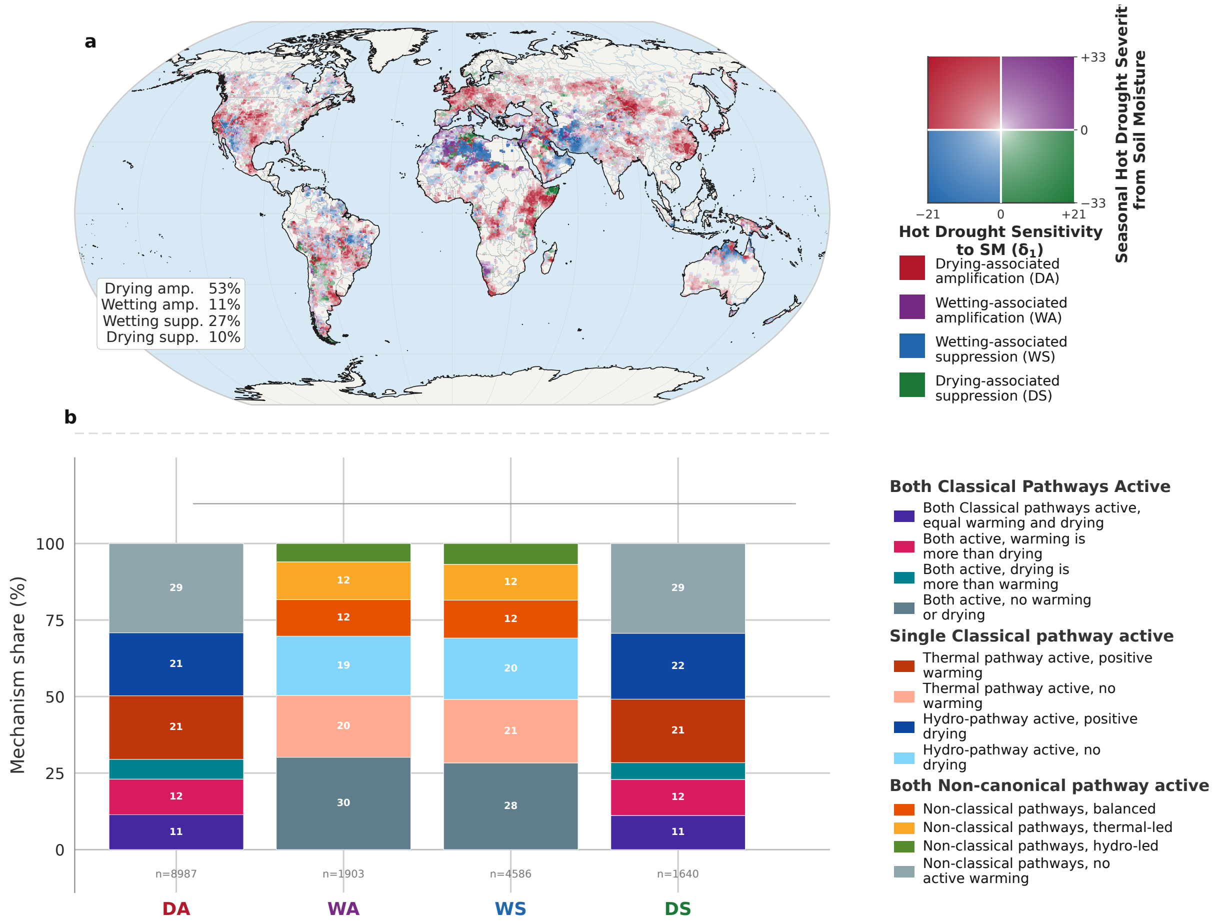

Supplementary Figure 4: Where and how strongly soil moisture is associated with hot drought severity in over the (a) globe in 2022 .Each grid cell is coloured by two quantities simultaneously: δ_1 and C_{SM}. Red (blue) tones indicate that dry (wet) soil is associated heat extremes. Color saturation reflects signal strength.(b) For each coupling regime identified in panels (a), the bars show what heterogenity in land-atmospheric feedback pathway of grid cells experienced.

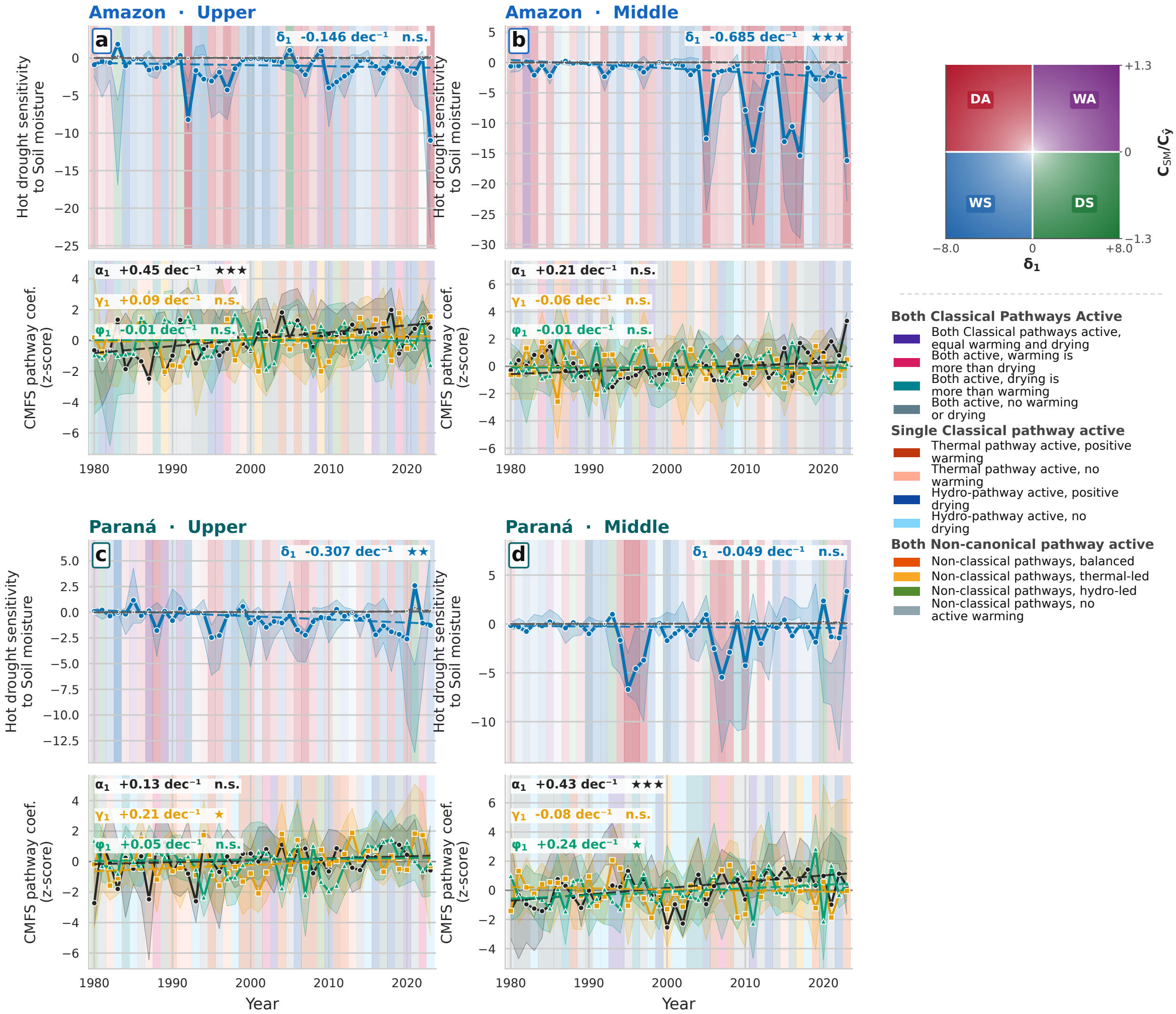

Supplementary Figure 5: (a–d) time series of soil-moisture-hot drought and land-atmospheric (CMFS) coupling coefficients for four river basin segments: Amazon Upper (a), Amazon Middle (b), Parana upper (c), Parana middle (d). Each panel pair shows two quantities.Upper sub-panel shows the sensitivity of hot drought severity to SM′ (δ_1, blue) with dashed lines showing Theil–Sen trends; background colour encodes the soil-hot drought coupling regime in each year. Lower sub-panel shows z-scored land–atmosphere pathway coefficients: sensitivity of evaporation to soil moisture (α_1), daily maximum temperature to evaporation (γ_1), and precipitation to evaporation (φ_1). Background shading indicates the LA feedback pathway in each year

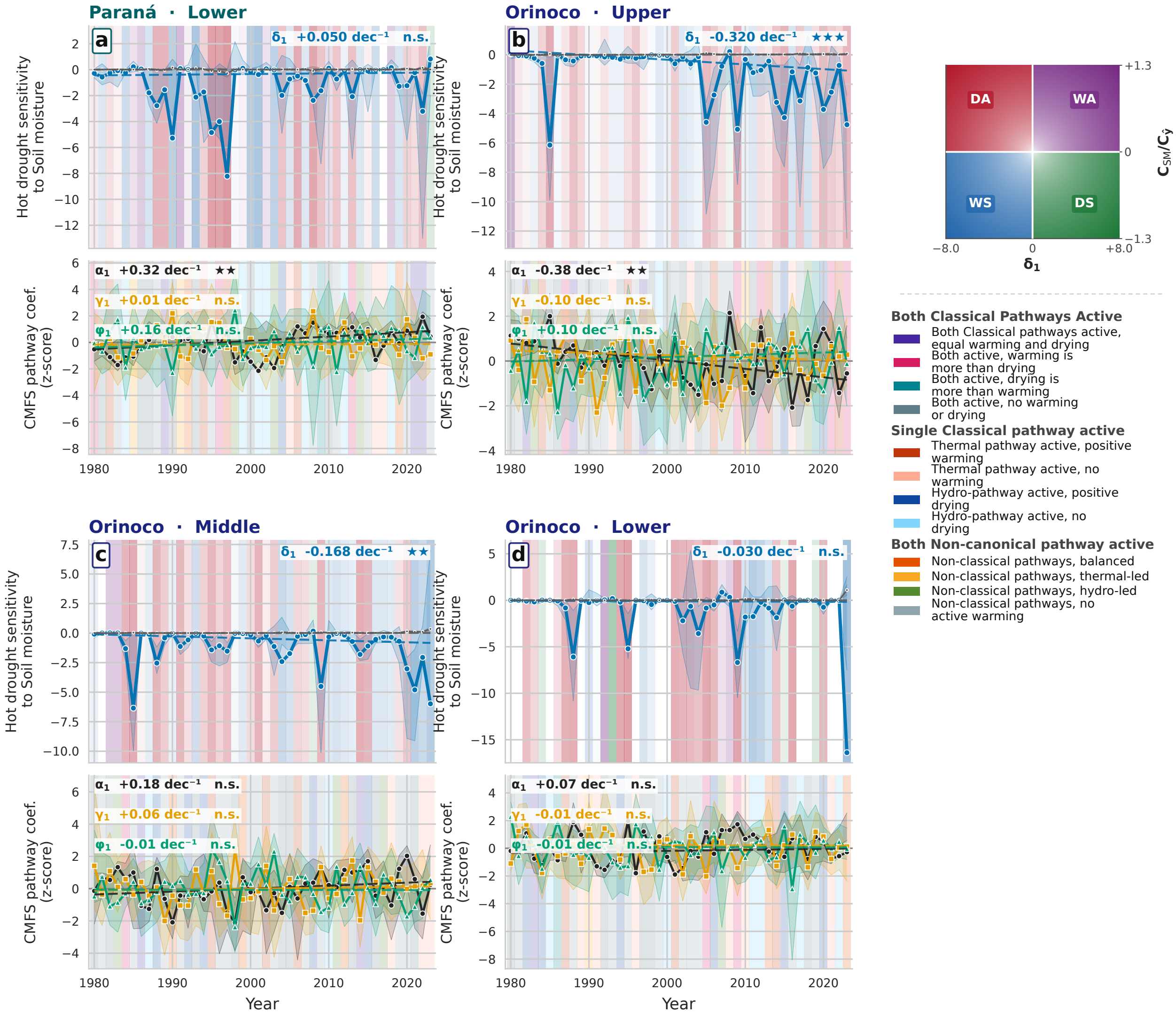

Supplementary Figure 6: (a–d) time series of soil-moisture-hot drought and land-atmospheric (CMFS) coupling coefficients for four river basin segments: Parana lower (a), Orinoco upper (b), Orinoco middle (c), Orinoco lower (d). Each panel pair shows two quantities.Upper sub-panel shows the sensitivity of hot drought severity to SM′ (δ_1, blue) with dashed lines showing Theil–Sen trends; background colour encodes the soil-hot drought coupling regime in each year. Lower sub-panel shows z-scored land–atmosphere pathway coefficients: sensitivity of evaporation to soil moisture (α_1), daily maximum temperature to evaporation (γ_1), and precipitation to evaporation (φ_1). Background shading indicates the LA feedback pathway in each year

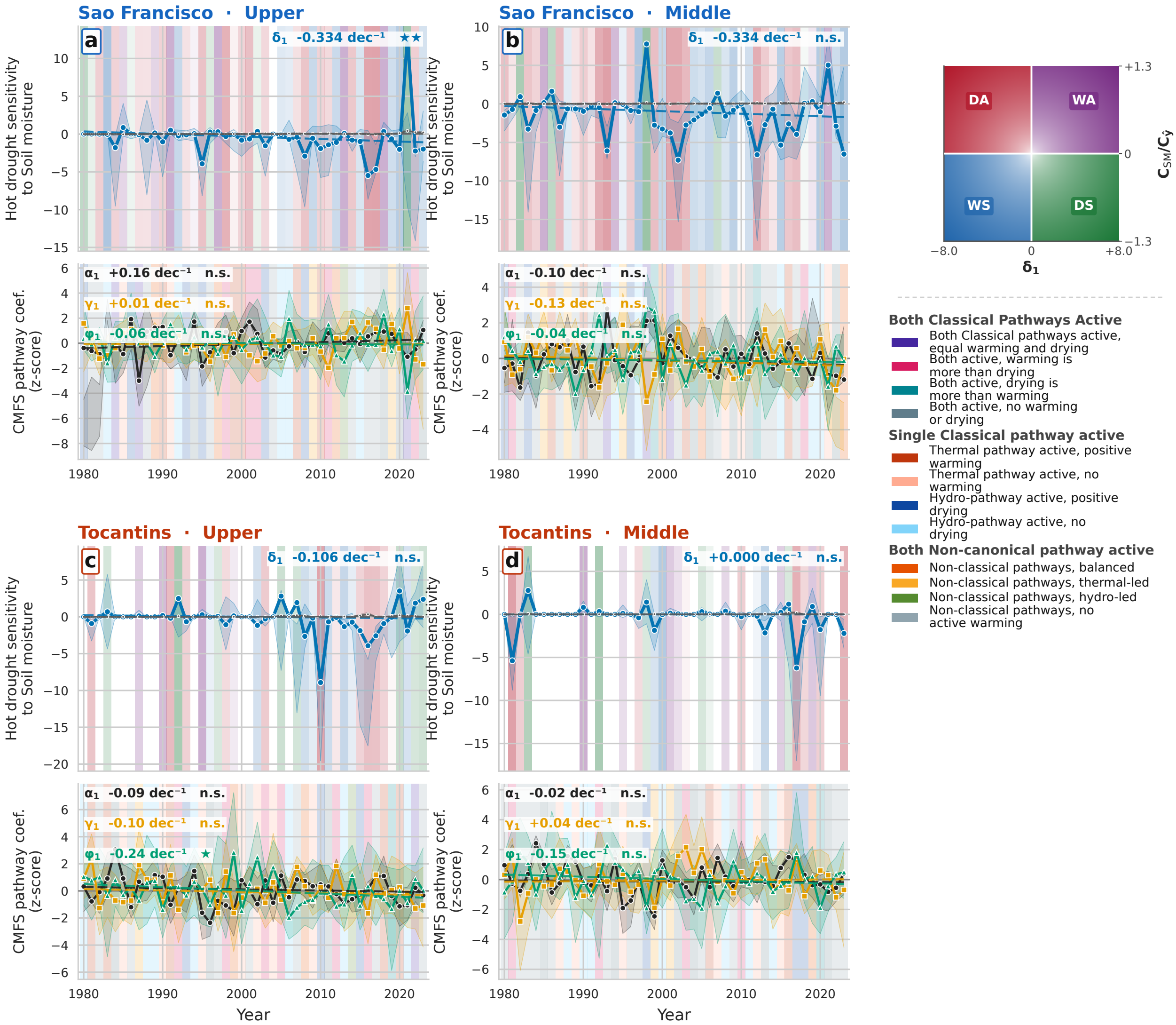

Supplementary Figure 7: (a–d) time series of soil-moisture-hot drought and land-atmospheric (CMFS) coupling coefficients for four river basin segments: Sao Francisco upper (a), Sao Francisco middle (b), Tocantins upper (c), Tocantins middle (d). Each panel pair shows two quantities.Upper sub-panel shows the sensitivity of hot drought severity to SM′ (δ_1, blue) with dashed lines showing Theil–Sen trends; background colour encodes the soil-hot drought coupling regime in each year. Lower sub-panel shows z-scored land–atmosphere pathway coefficients: sensitivity of evaporation to soil moisture (α_1), daily maximum temperature to evaporation (γ_1), and precipitation to evaporation (φ_1). Background shading indicates the LA feedback pathway in each year

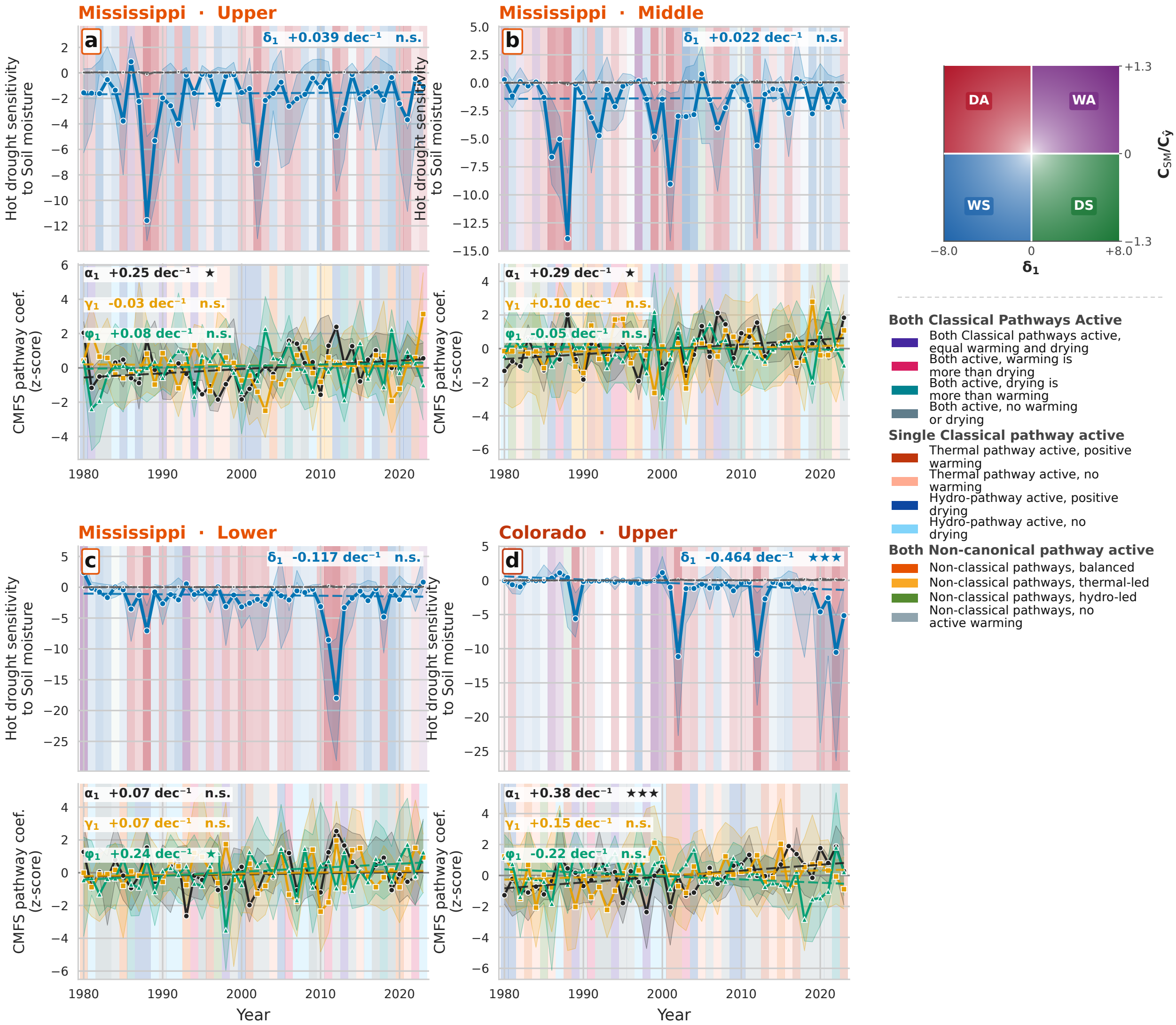

Supplementary Figure 8: (a–d) time series of soil-moisture-hot drought and land-atmospheric (CMFS) coupling coefficients for four river basin segments: Mississippi upper (a), Mississippi middle (b), Mississippi lower (c), Colorado upper (d). Each panel pair shows two quantities.Upper sub-panel shows the sensitivity of hot drought severity to SM′ (δ_1, blue) with dashed lines showing Theil–Sen trends; background colour encodes the soil-hot drought coupling regime in each year. Lower sub-panel shows z-scored land–atmosphere pathway coefficients: sensitivity of evaporation to soil moisture (α_1), daily maximum temperature to evaporation (γ_1), and precipitation to evaporation (φ_1). Background shading indicates the LA feedback pathway in each year

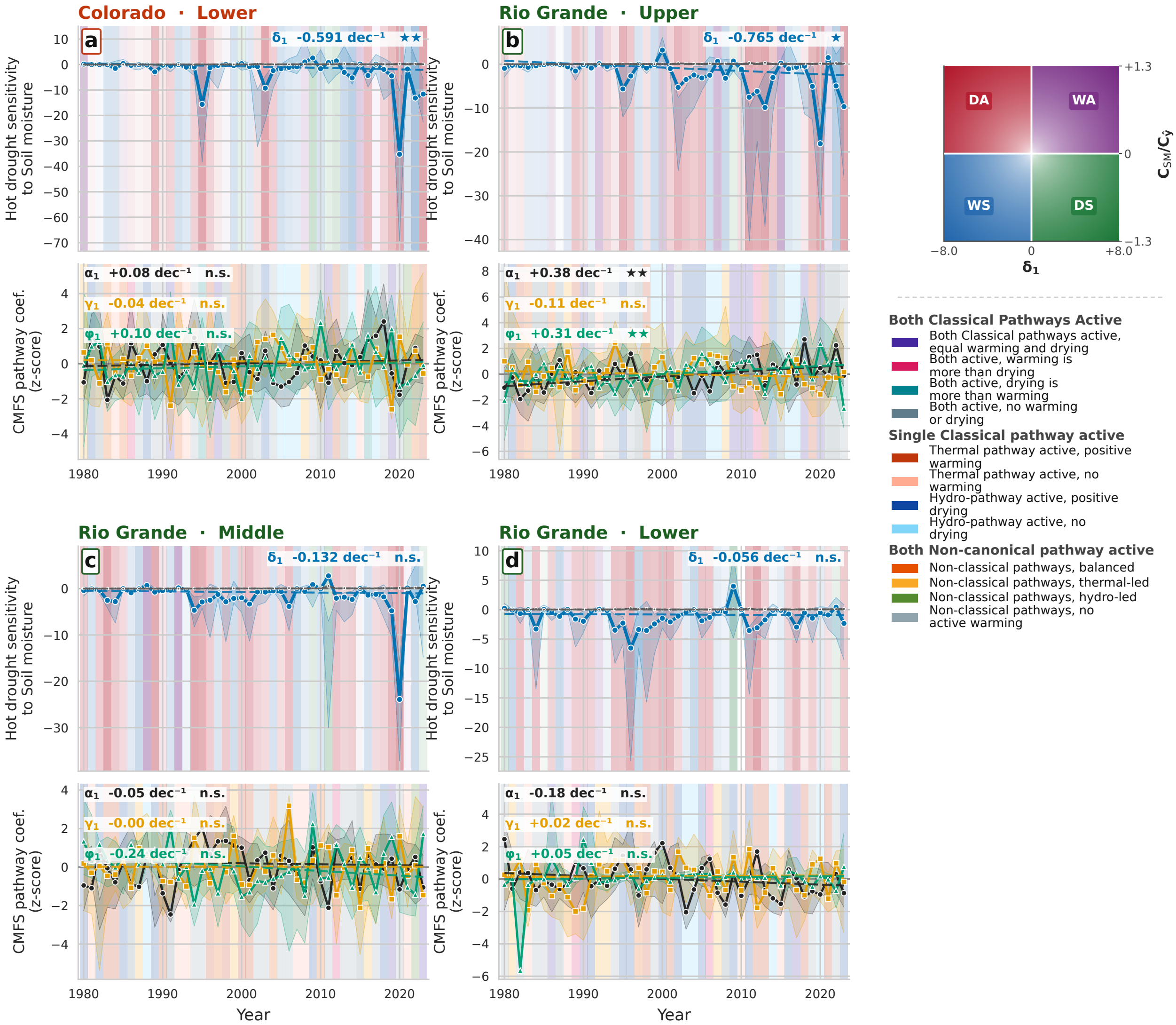

Supplementary Figure 9: (a–d) time series of soil-moisture-hot drought and land-atmospheric (CMFS) coupling coefficients for four river basin segments: Colorado lower (a), Rio grande Upper (b), Riograde middle (c), Riogrande lower(d). Each panel pair shows two quantities.Upper sub-panel shows the sensitivity of hot drought severity to SM′ (δ_1, blue) with dashed lines showing Theil–Sen trends; background colour encodes the soil-hot drought coupling regime in each year. Lower sub-panel shows z-scored land–atmosphere pathway coefficients: sensitivity of evaporation to soil moisture (α_1), daily maximum temperature to evaporation (γ_1), and precipitation to evaporation (φ_1). Background shading indicates the LA feedback pathway in each year

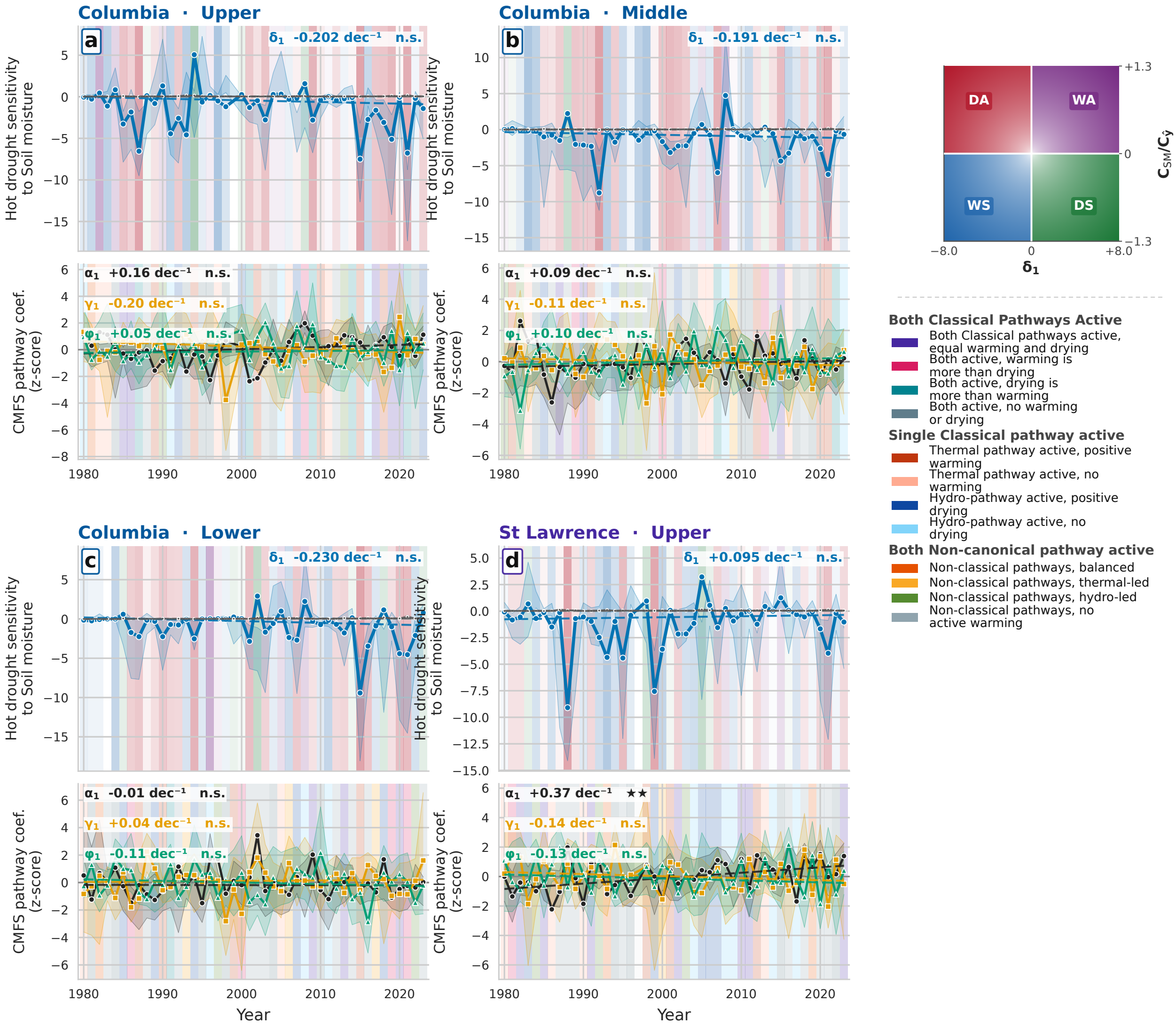

Supplementary Figure 10: (a–d) time series of soil-moisture-hot drought and land-atmospheric (CMFS) coupling coefficients for four river basin segments: Columbia Upper (a), Columbia middle (b), Columbia Upper (c), St. Lawrence Upper(d). Each panel pair shows two quantities.Upper sub-panel shows the sensitivity of hot drought severity to SM′ (δ_1, blue) with dashed lines showing Theil–Sen trends; background colour encodes the soil-hot drought coupling regime in each year. Lower sub-panel shows z-scored land–atmosphere pathway coefficients: sensitivity of evaporation to soil moisture (α_1), daily maximum temperature to evaporation (γ_1), and precipitation to evaporation (φ_1). Background shading indicates the LA feedback pathway in each year

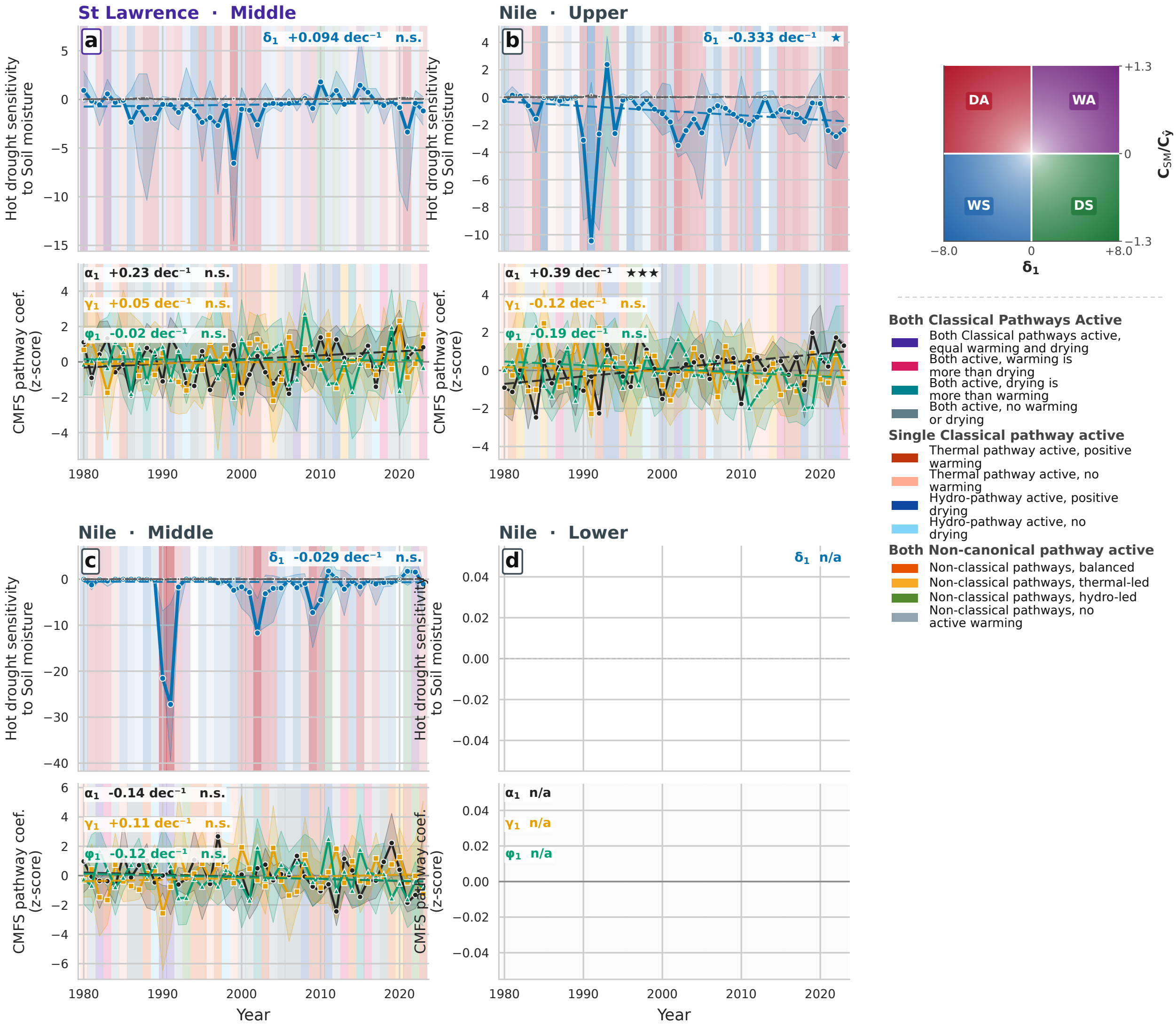

Supplementary Figure 11: (a–d) time series of soil-moisture-hot drought and land-atmospheric (CMFS) coupling coefficients for four river basin segments: St. Lawrence middle (a), Nile Upper (b), Nile middle (c), Nile lower(d). Each panel pair shows two quantities.Upper sub-panel shows the sensitivity of hot drought severity to SM′ (δ_1, blue) with dashed lines showing Theil–Sen trends; background colour encodes the soil-hot drought coupling regime in each year. Lower sub-panel shows z-scored land–atmosphere pathway coefficients: sensitivity of evaporation to soil moisture (α_1), daily maximum temperature to evaporation (γ_1), and precipitation to evaporation (φ_1). Background shading indicates the LA feedback pathway in each year

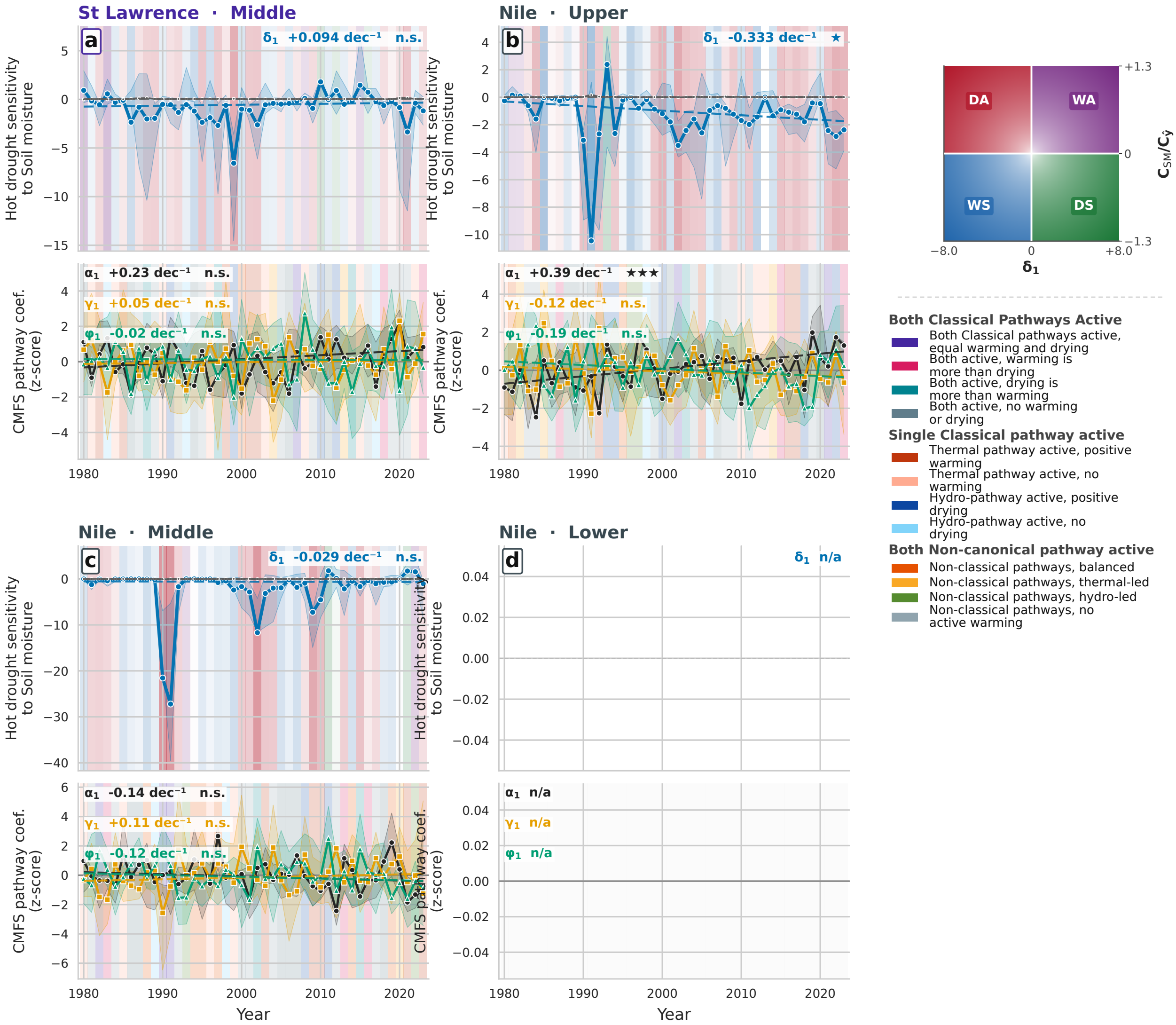

Supplementary Figure 12: (a–d) time series of soil-moisture-hot drought and land-atmospheric (CMFS) coupling coefficients for four river basin segments: St. Lawrence middle (a), Nile Upper (b), Nile middle (c), Nile lower(d). Each panel pair shows two quantities.Upper sub-panel shows the sensitivity of hot drought severity to SM′ (δ_1, blue) with dashed lines showing Theil–Sen trends; background colour encodes the soil-hot drought coupling regime in each year. Lower sub-panel shows z-scored land–atmosphere pathway coefficients: sensitivity of evaporation to soil moisture (α_1), daily maximum temperature to evaporation (γ_1), and precipitation to evaporation (φ_1). Background shading indicates the LA feedback pathway in each year

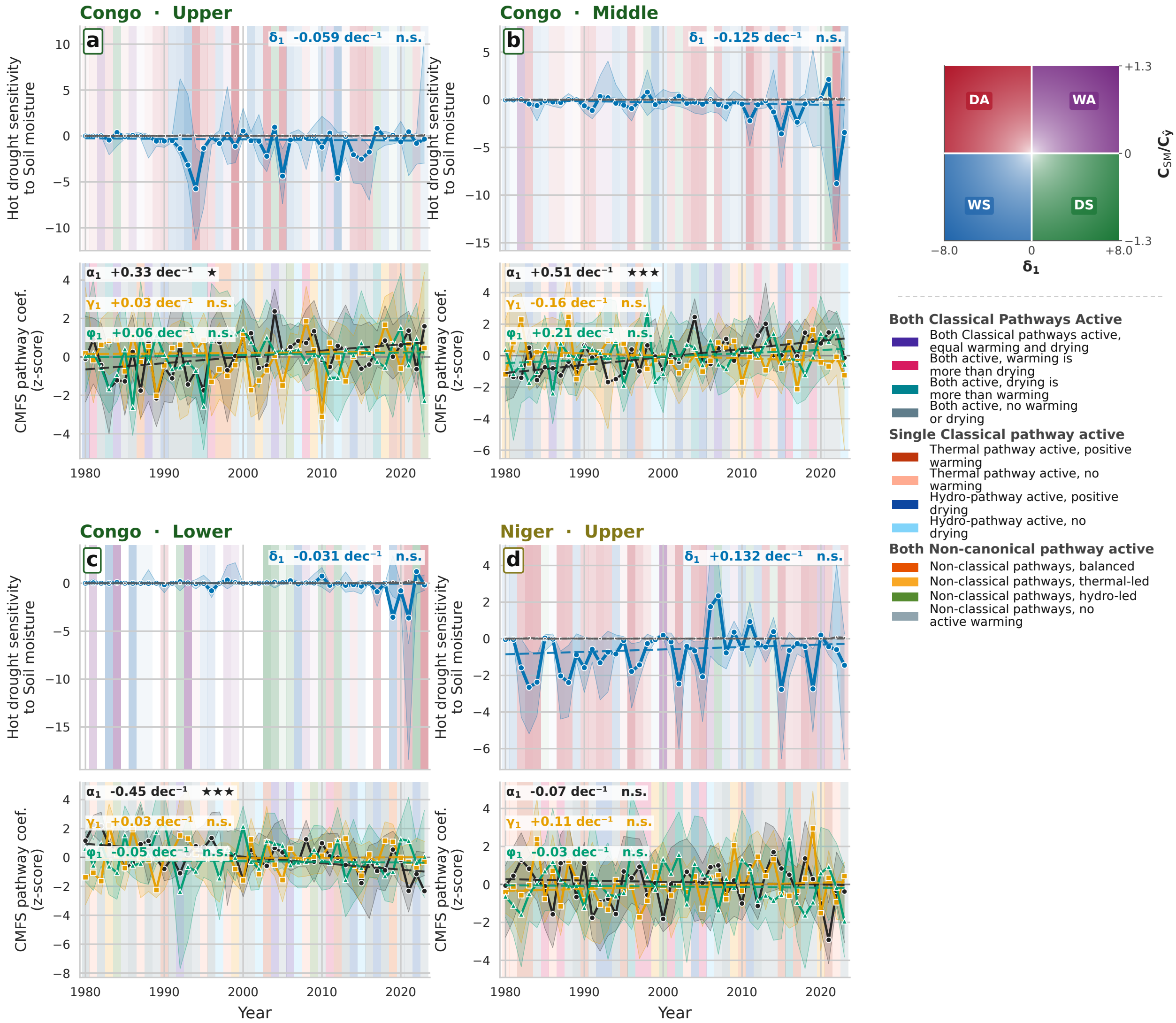

Supplementary Figure 13: (a–d) time series of soil-moisture-hot drought and land-atmospheric (CMFS) coupling coefficients for four river basin segments: Congo upper (a), Congo middle (b), Congo lower (c), Niger Upper(d). Each panel pair shows two quantities.Upper sub-panel shows the sensitivity of hot drought severity to SM′ (δ_1, blue) with dashed lines showing Theil–Sen trends; background colour encodes the soil-hot drought coupling regime in each year. Lower sub-panel shows z-scored land–atmosphere pathway coefficients: sensitivity of evaporation to soil moisture (α_1), daily maximum temperature to evaporation (γ_1), and precipitation to evaporation (φ_1). Background shading indicates the LA feedback pathway in each year

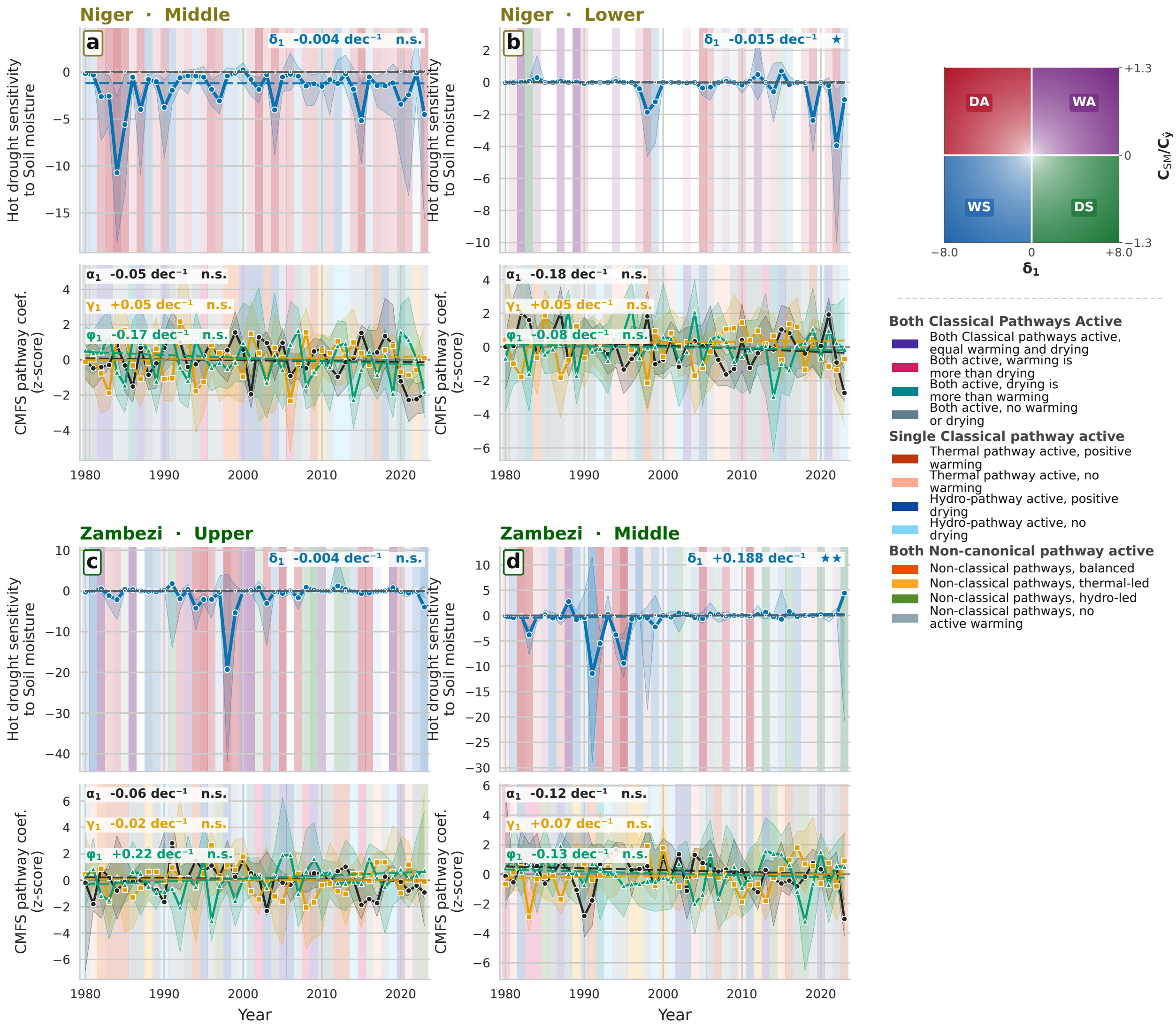

Supplementary Figure 14: (a–d) time series of soil-moisture-hot drought and land-atmospheric (CMFS) coupling coefficients for four river basin segments: Niger middle (a), Niger Lower (b), Zambeji upper (c), Zambeji middle(d). Each panel pair shows two quantities.Upper sub-panel shows the sensitivity of hot drought severity to SM′ (δ_1, blue) with dashed lines showing Theil–Sen trends; background colour encodes the soil-hot drought coupling regime in each year. Lower sub-panel shows z-scored land–atmosphere pathway coefficients: sensitivity of evaporation to soil moisture (α_1), daily maximum temperature to evaporation (γ_1), and precipitation to evaporation (φ_1). Background shading indicates the LA feedback pathway in each year

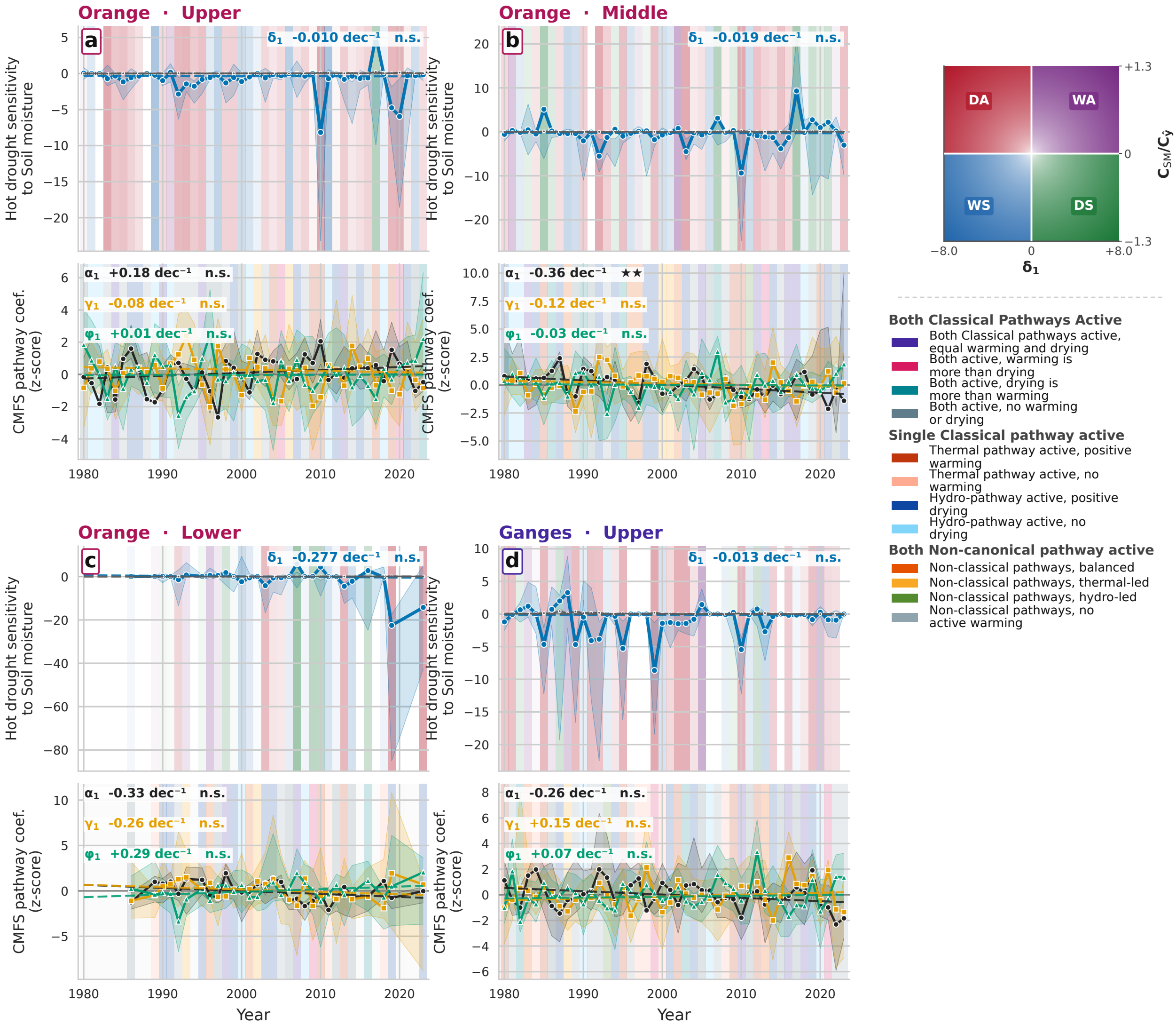

Supplementary Figure 15: (a–d) time series of soil-moisture-hot drought and land-atmospheric (CMFS) coupling coefficients for four river basin segments: Orange upper (a), Orange middle (b), Orange lower (c), Ganges upper(d). Each panel pair shows two quantities.Upper sub-panel shows the sensitivity of hot drought severity to SM′ (δ_1, blue) with dashed lines showing Theil–Sen trends; background colour encodes the soil-hot drought coupling regime in each year. Lower sub-panel shows z-scored land–atmosphere pathway coefficients: sensitivity of evaporation to soil moisture (α_1), daily maximum temperature to evaporation (γ_1), and precipitation to evaporation (φ_1). Background shading indicates the LA feedback pathway in each year

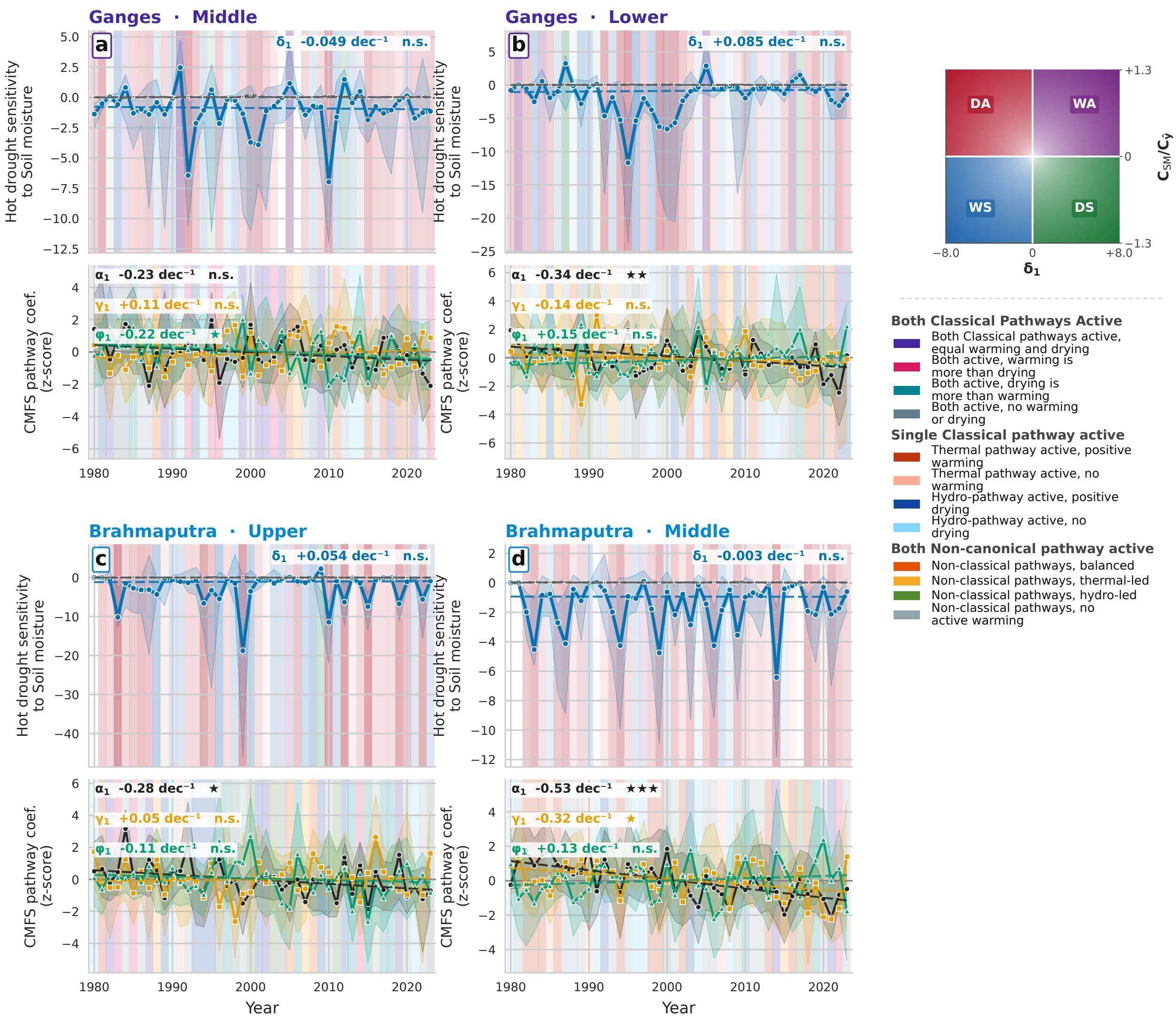

Supplementary Figure 16: (a–d) time series of soil-moisture-hot drought and land-atmospheric (CMFS) coupling coefficients for four river basin segments: Ganges middle (a), Ganges Lower (b), Brahmaputra upper (c), Brahmaputra middle (d). Each panel pair shows two quantities.Upper sub-panel shows the sensitivity of hot drought severity to SM′ (δ_1, blue) with dashed lines showing Theil–Sen trends; background colour encodes the soil-hot drought coupling regime in each year. Lower sub-panel shows z-scored land–atmosphere pathway coefficients: sensitivity of evaporation to soil moisture (α_1), daily maximum temperature to evaporation (γ_1), and precipitation to evaporation (φ_1). Background shading indicates the LA feedback pathway in each year

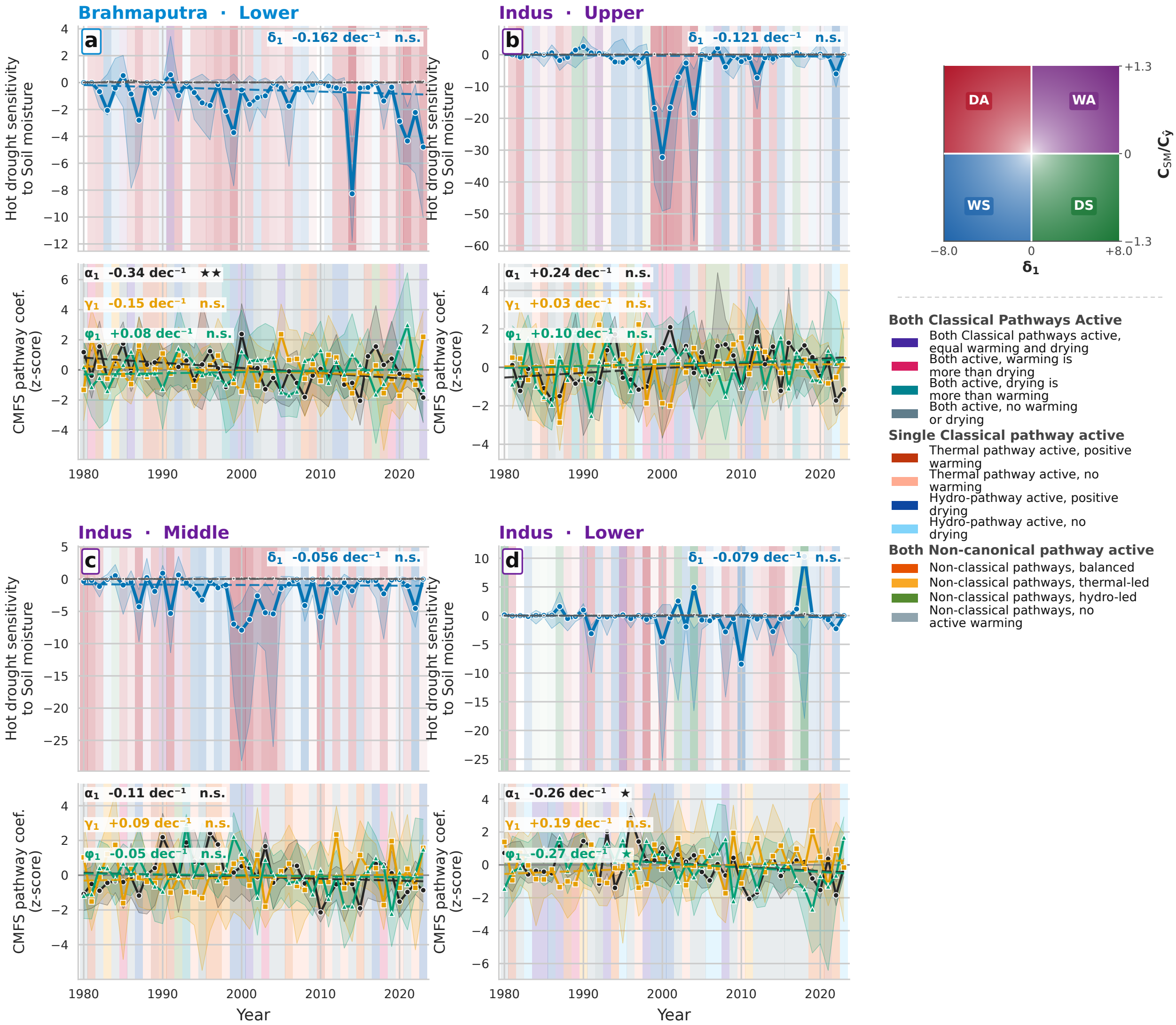

Supplementary Figure 17: (a–d) time series of soil-moisture-hot drought and land-atmospheric (CMFS) coupling coefficients for four river basin segments: Brahmaputra lower (a), Indus upper (b), Indus middle (c), Indus lower (d). Each panel pair shows two quantities.Upper sub-panel shows the sensitivity of hot drought severity to SM′ (δ_1, blue) with dashed lines showing Theil–Sen trends; background colour encodes the soil-hot drought coupling regime in each year. Lower sub-panel shows z-scored land–atmosphere pathway coefficients: sensitivity of evaporation to soil moisture (α_1), daily maximum temperature to evaporation (γ_1), and precipitation to evaporation (φ_1). Background shading indicates the LA feedback pathway in each year

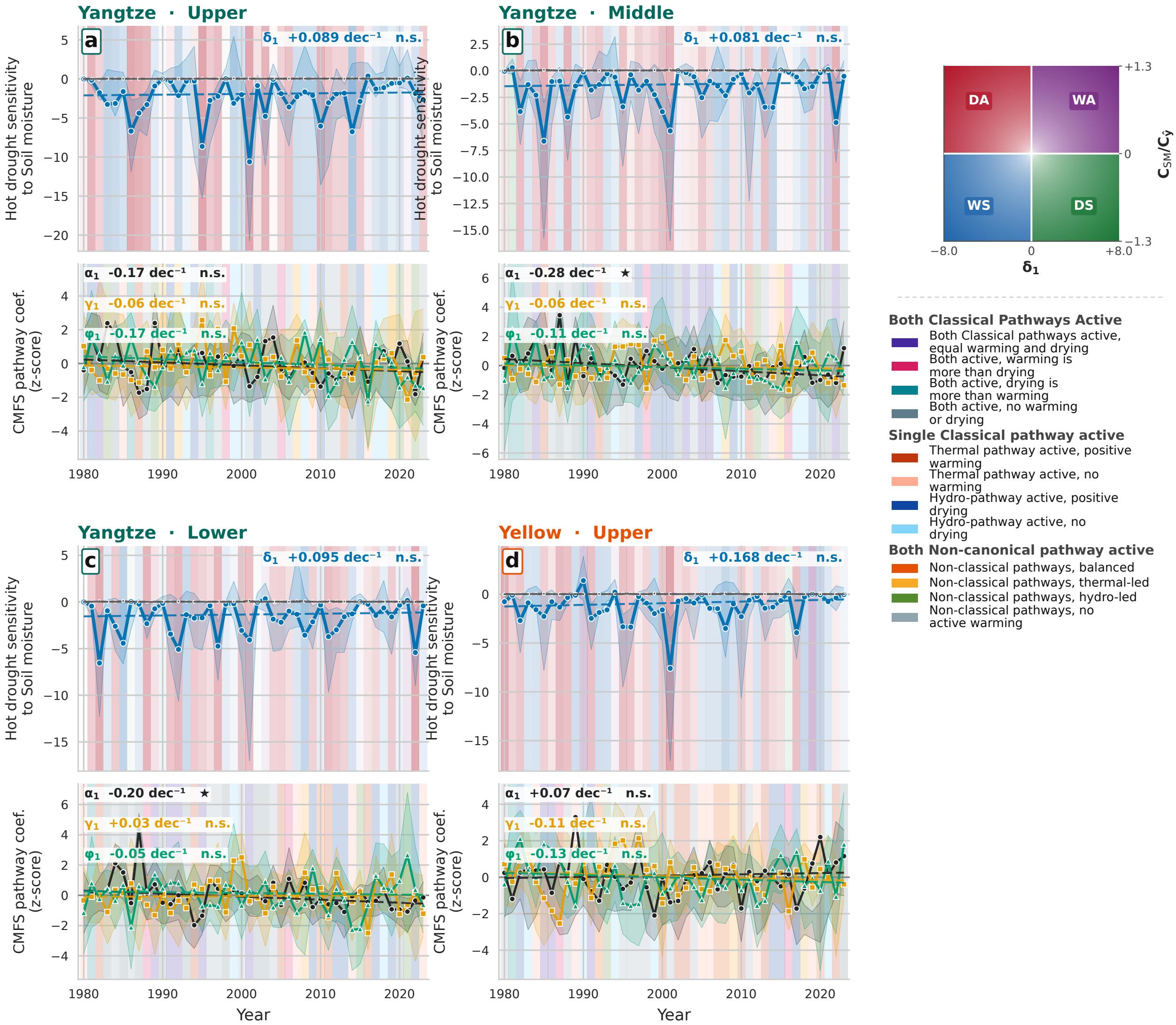

Supplementary Figure 18: (a–d) time series of soil-moisture-hot drought and land-atmospheric (CMFS) coupling coefficients for four river basin segments: Yangtze upper (a), Yangtze middle (b), Yangtze lower (c), Yellow upper(d). Each panel pair shows two quantities.Upper sub-panel shows the sensitivity of hot drought severity to SM′ (δ_1, blue) with dashed lines showing Theil–Sen trends; background colour encodes the soil-hot drought coupling regime in each year. Lower sub-panel shows z-scored land–atmosphere pathway coefficients: sensitivity of evaporation to soil moisture (α_1), daily maximum temperature to evaporation (γ_1), and precipitation to evaporation (φ_1). Background shading indicates the LA feedback pathway in each year

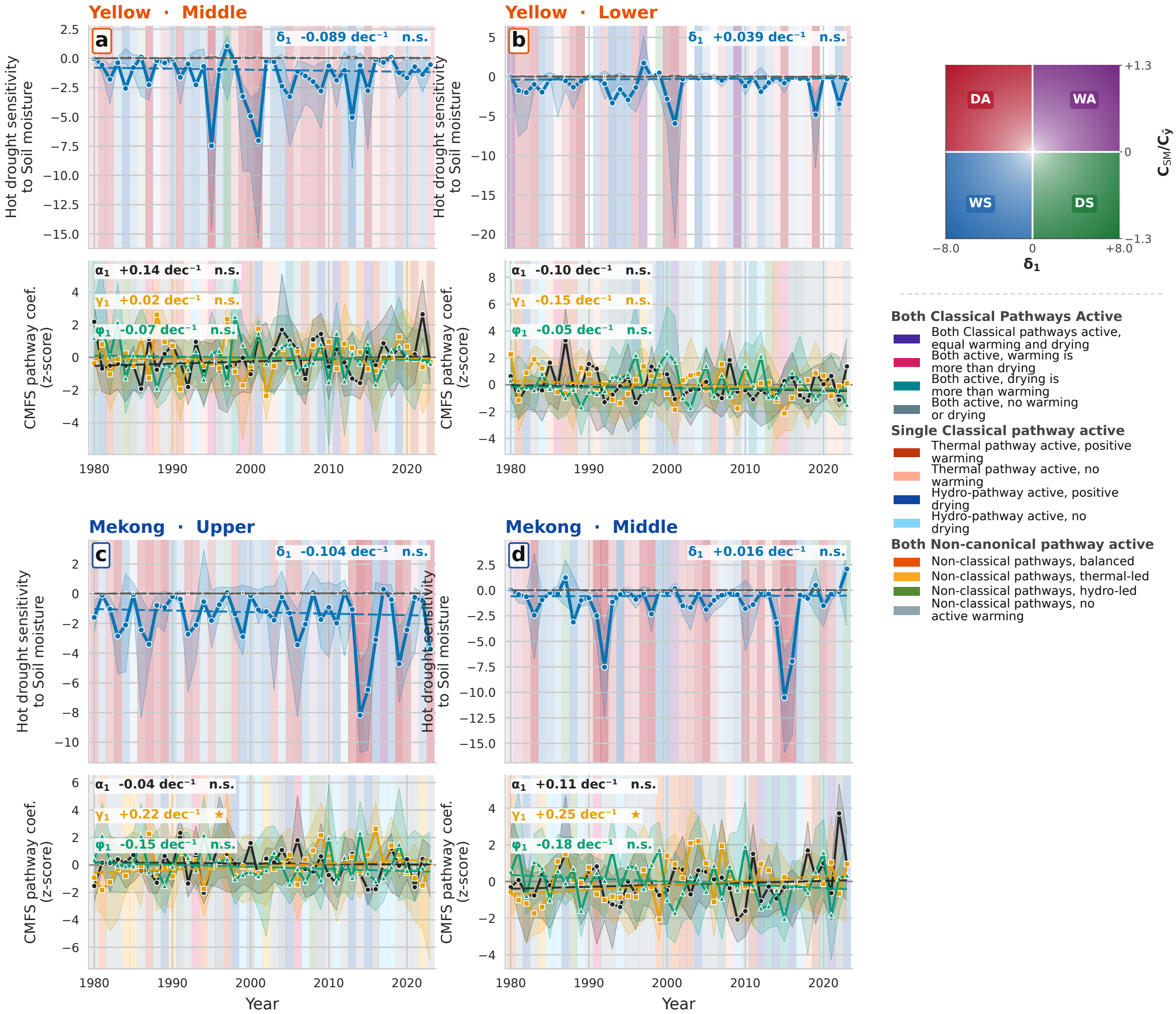

Supplementary Figure 19: (a–d) time series of soil-moisture-hot drought and land-atmospheric (CMFS) coupling coefficients for four river basin segments: Yellow middle (a), Yellow lower (b), Mekong upper (c), Mekong middle(d). Each panel pair shows two quantities.Upper sub-panel shows the sensitivity of hot drought severity to SM′ (δ_1, blue) with dashed lines showing Theil–Sen trends; background colour encodes the soil-hot drought coupling regime in each year. Lower sub-panel shows z-scored land–atmosphere pathway coefficients: sensitivity of evaporation to soil moisture (α_1), daily maximum temperature to evaporation (γ_1), and precipitation to evaporation (φ_1). Background shading indicates the LA feedback pathway in each year

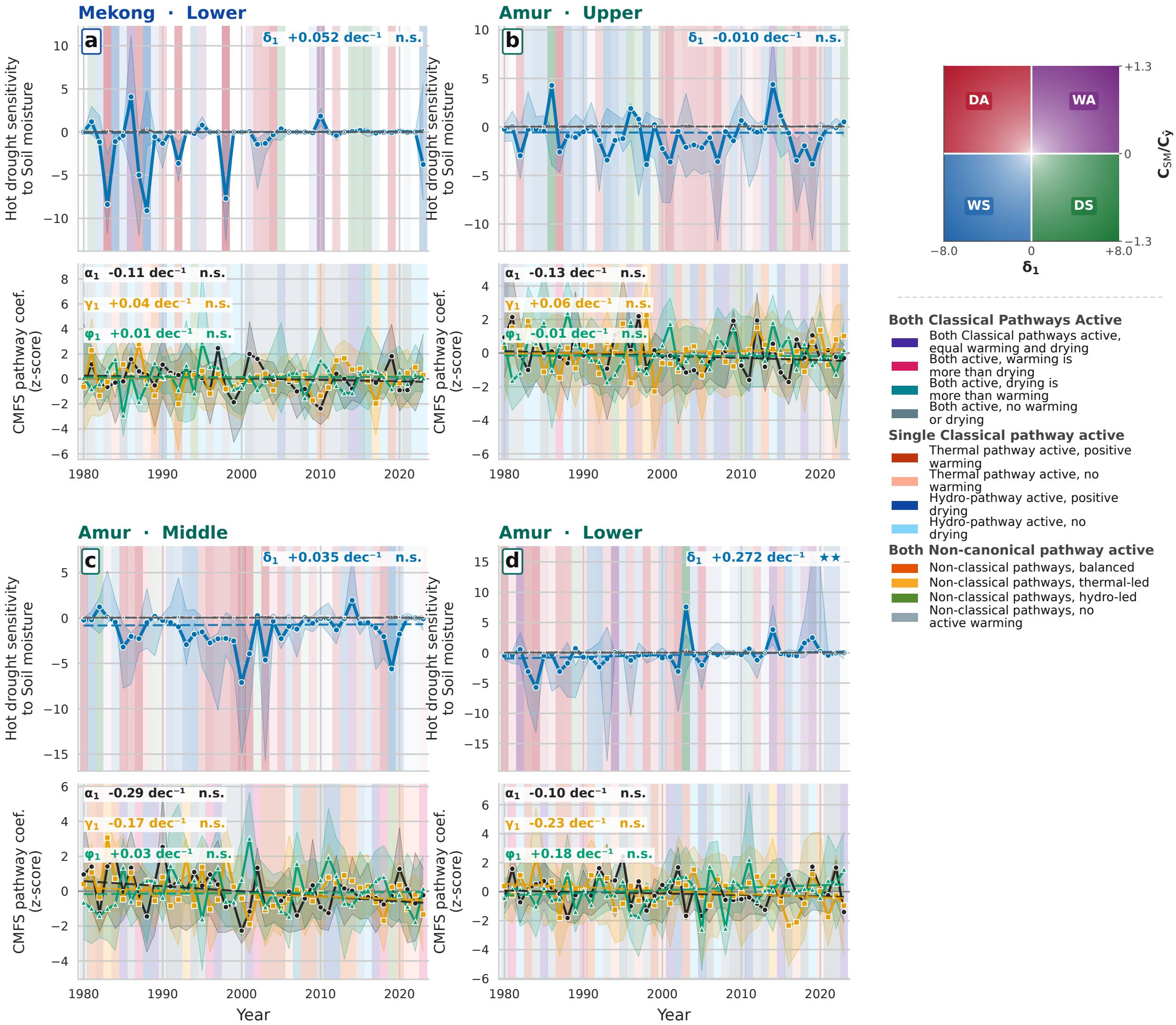

Supplementary Figure 20: (a–d) time series of soil-moisture-hot drought and land-atmospheric (CMFS) coupling coefficients for four river basin segments: Mekong lower (a), Amur upper (b), Amur middle (c), Amur lower(d). Each panel pair shows two quantities.Upper sub-panel shows the sensitivity of hot drought severity to SM′ (δ_1, blue) with dashed lines showing Theil–Sen trends; background colour encodes the soil-hot drought coupling regime in each year. Lower sub-panel shows z-scored land–atmosphere pathway coefficients: sensitivity of evaporation to soil moisture (α_1), daily maximum temperature to evaporation (γ_1), and precipitation to evaporation (φ_1). Background shading indicates the LA feedback pathway in each year

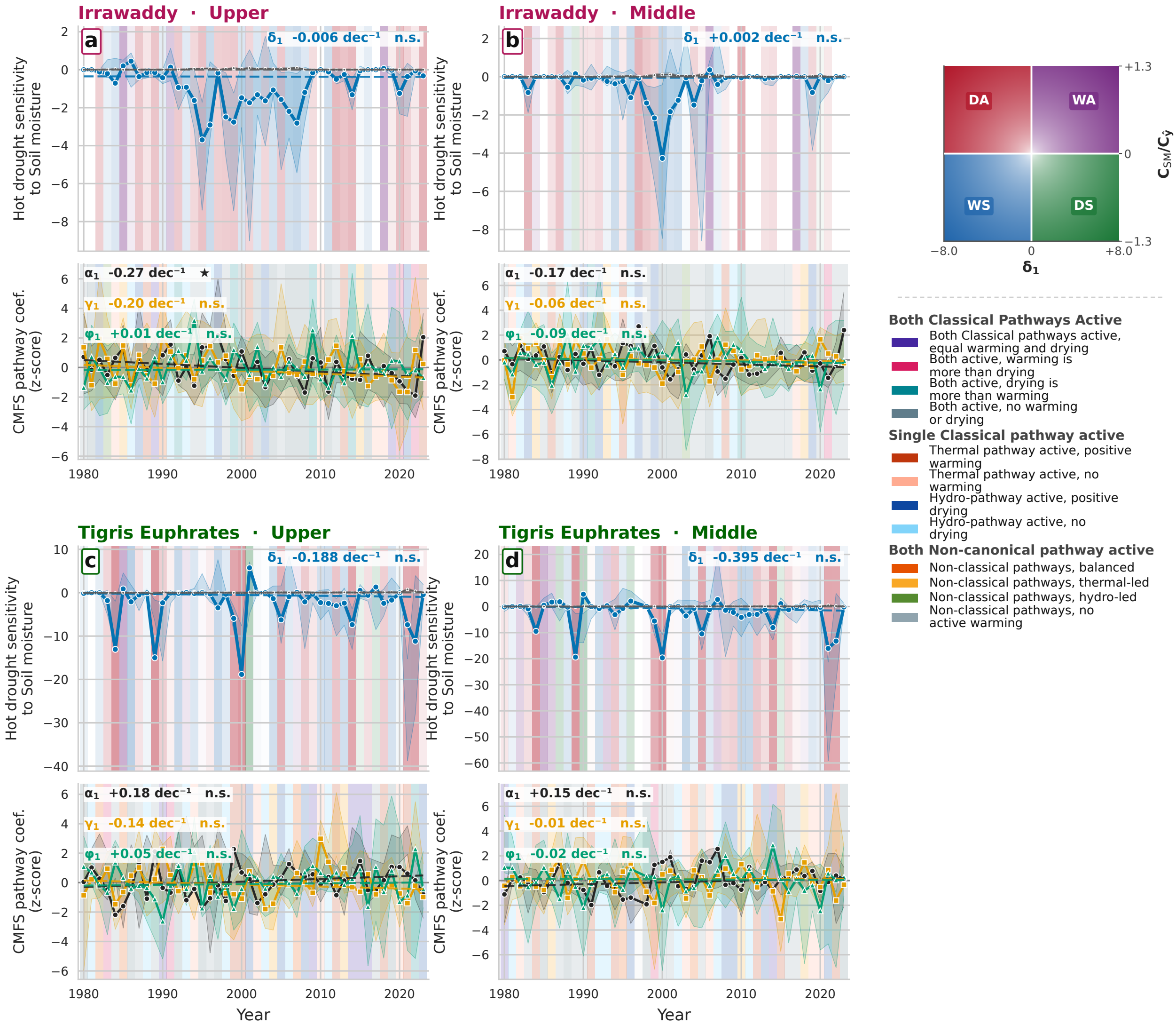

Supplementary Figure 21: (a–d) time series of soil-moisture-hot drought and land-atmospheric (CMFS) coupling coefficients for four river basin segments: Irrawaddy upper (a), Irrawaddy middle (b), Tigris Euphrates Upper(c), Tigris Euphrates Middle(d). Each panel pair shows two quantities.Upper sub-panel shows the sensitivity of hot drought severity to SM′ (δ_1, blue) with dashed lines showing Theil–Sen trends; background colour encodes the soil-hot drought coupling regime in each year. Lower sub-panel shows z-scored land–atmosphere pathway coefficients: sensitivity of evaporation to soil moisture (α_1), daily maximum temperature to evaporation (γ_1), and precipitation to evaporation (φ_1). Background shading indicates the LA feedback pathway in each year

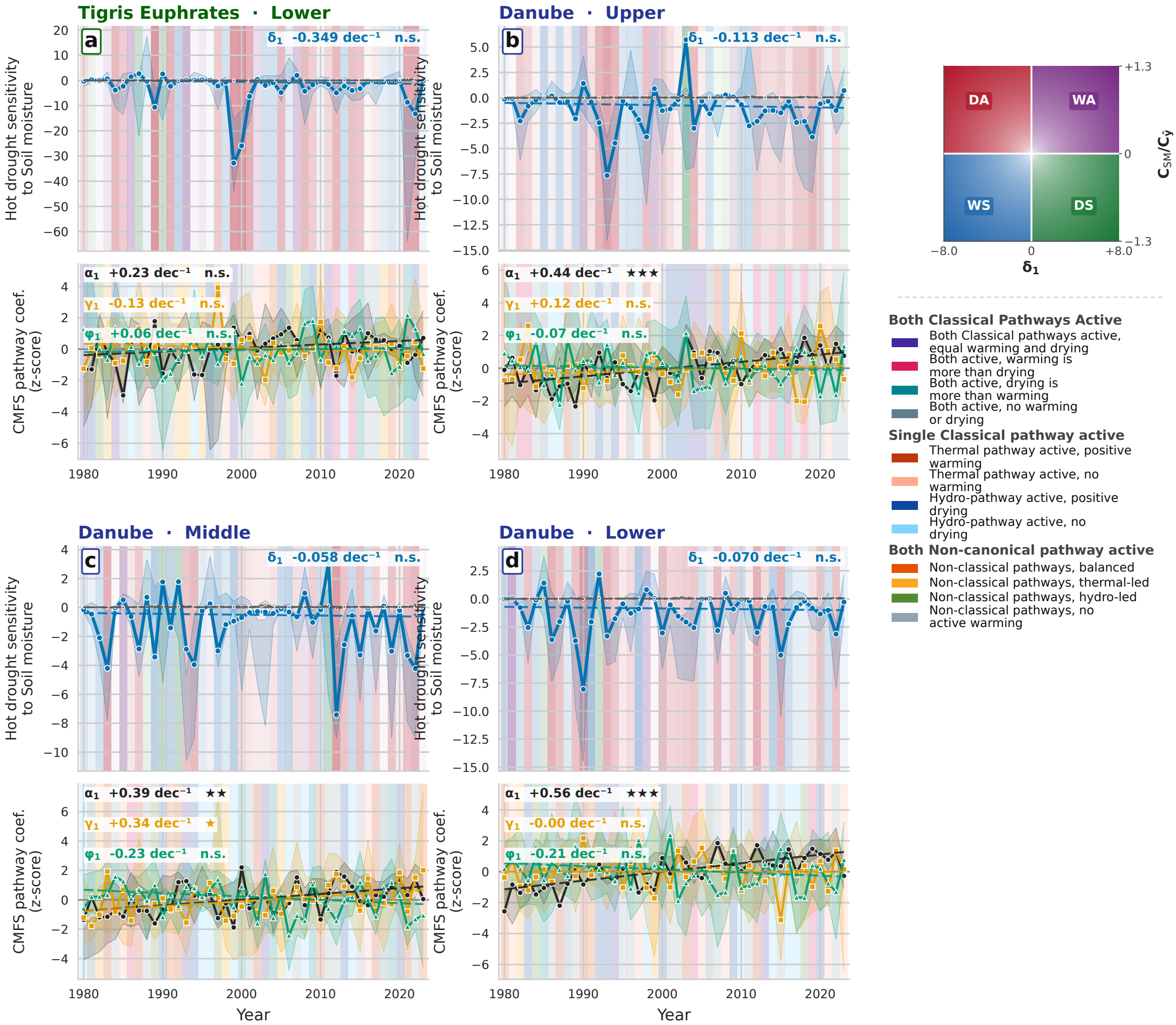

Supplementary Figure 22: (a–d) time series of soil-moisture-hot drought and land-atmospheric (CMFS) coupling coefficients for four river basin segments: Tigris and Euphrates lower (a), Danube upper (b), Danube middle (c), Danube lower(d). Each panel pair shows two quantities.Upper sub-panel shows the sensitivity of hot drought severity to SM′ (δ_1, blue) with dashed lines showing Theil–Sen trends; background colour encodes the soil-hot drought coupling regime in each year. Lower sub-panel shows z-scored land–atmosphere pathway coefficients: sensitivity of evaporation to soil moisture (α_1), daily maximum temperature to evaporation (γ_1), and precipitation to evaporation (φ_1). Background shading indicates the LA feedback pathway in each year

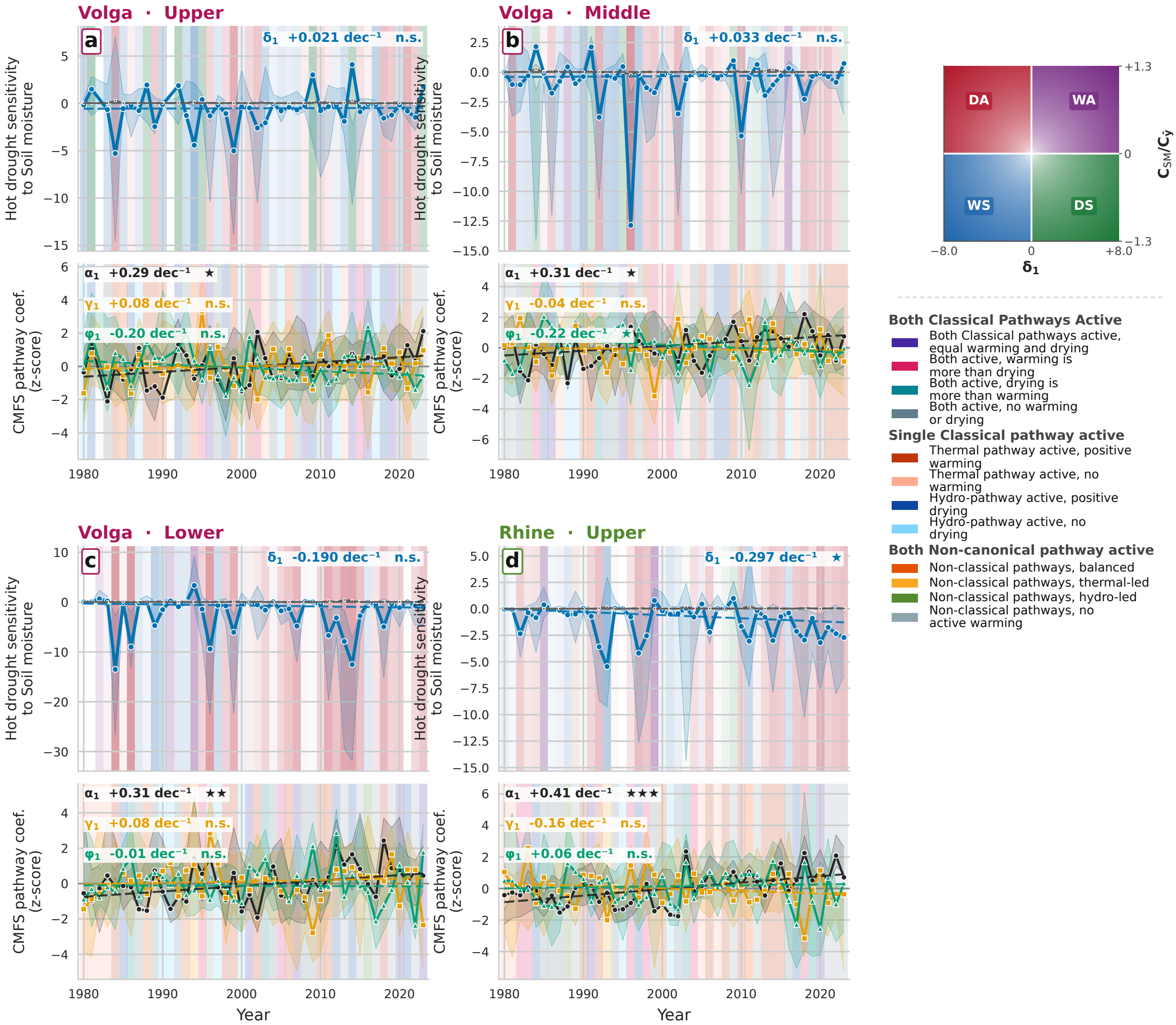

Supplementary Figure 23: (a–d) time series of soil-moisture-hot drought and land-atmospheric (CMFS) coupling coefficients for four river basin segments: Volga upper (a), Volga middle (b), Volga upper (c), Rhine upper (d). Each panel pair shows two quantities.Upper sub-panel shows the sensitivity of hot drought severity to SM′ (δ_1, blue) with dashed lines showing Theil–Sen trends; background colour encodes the soil-hot drought coupling regime in each year. Lower sub-panel shows z-scored land–atmosphere pathway coefficients: sensitivity of evaporation to soil moisture (α_1), daily maximum temperature to evaporation (γ_1), and precipitation to evaporation (φ_1). Background shading indicates the LA feedback pathway in each year

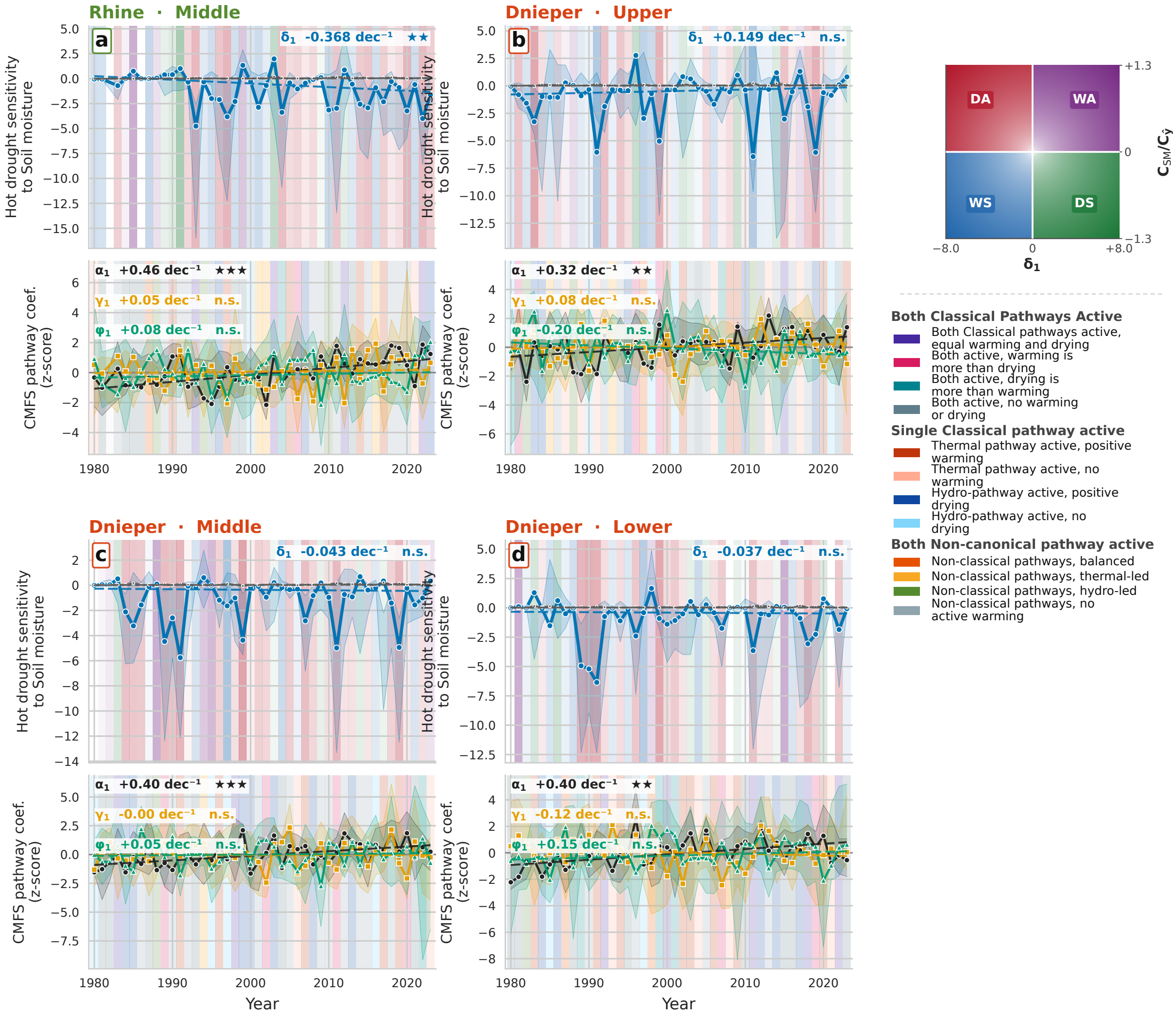

Supplementary Figure 24: (a–d) time series of soil-moisture-hot drought and land-atmospheric (CMFS) coupling coefficients for four river basin segments: Rhine middle (a), Dneiper upper (b), Deniper middle (c), Dneiper lower (d). Each panel pair shows two quantities.Upper sub-panel shows the sensitivity of hot drought severity to SM′ (δ_1, blue) with dashed lines showing Theil–Sen trends; background colour encodes the soil-hot drought coupling regime in each year. Lower sub-panel shows z-scored land–atmosphere pathway coefficients: sensitivity of evaporation to soil moisture (α_1), daily maximum temperature to evaporation (γ_1), and precipitation to evaporation (φ_1). Background shading indicates the LA feedback pathway in each year

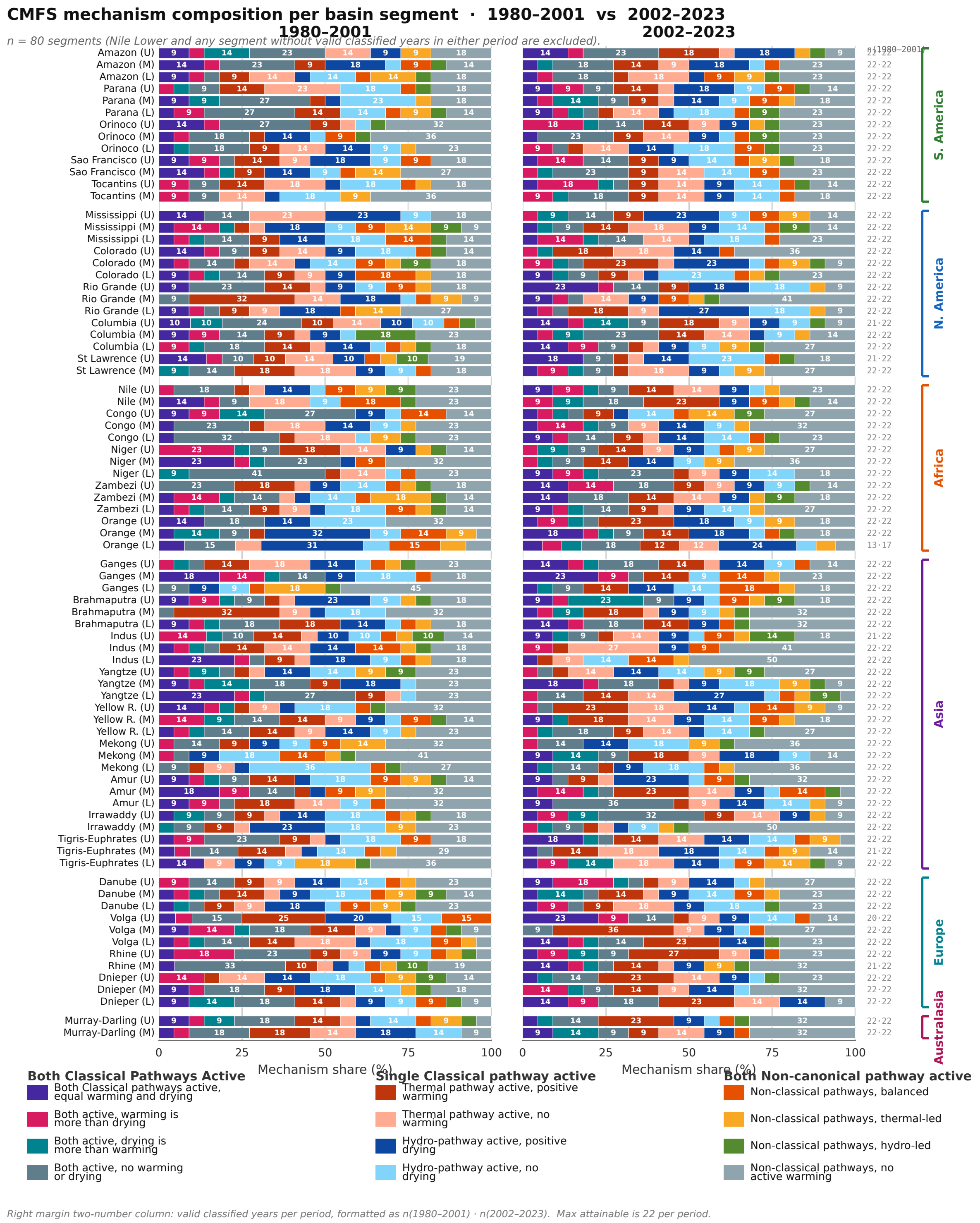

Supplementary Figure 25: Comparison of percentage distribution of land-atmospheric pathways between 2002-2023 with that of 1980-2001

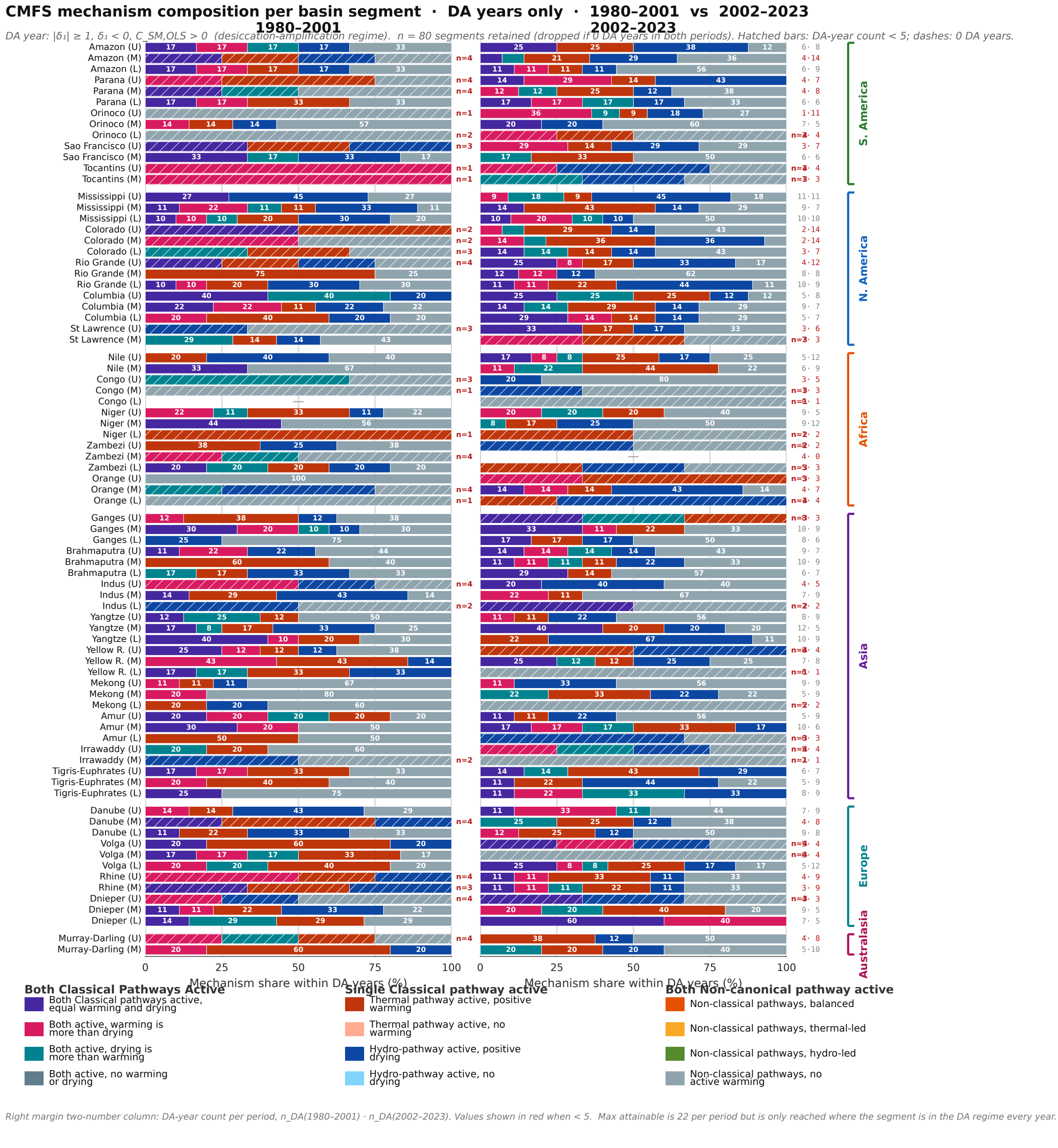

Supplementary Figure 26: Comparison of percentage distribution of land-atmospheric pathways in years when $SM - HD$ coupling is drying associated ampplification (DA) between 2002-2023 with that of 1980-2001

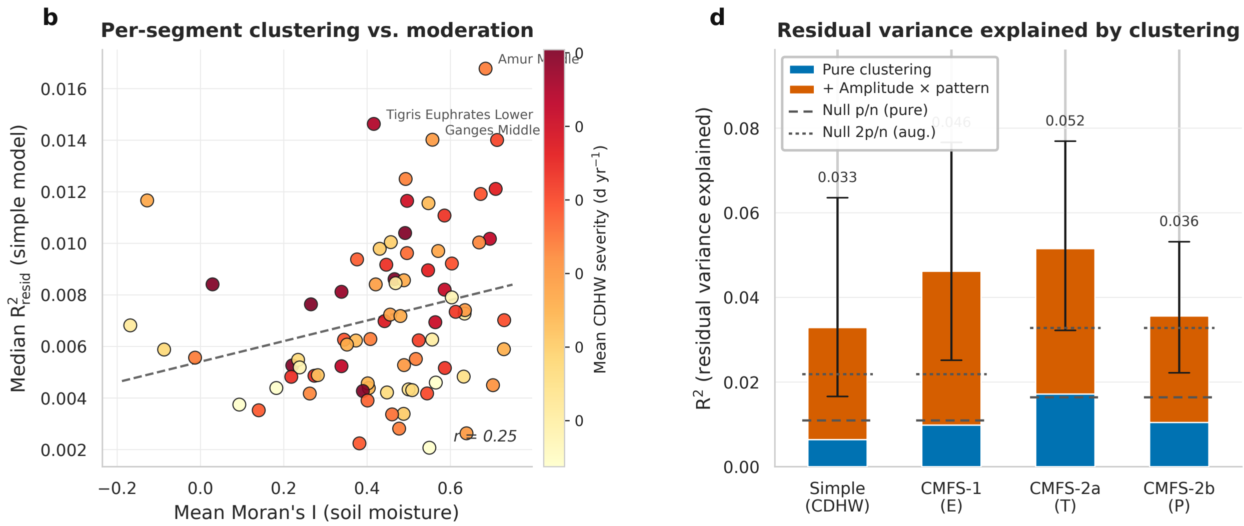

Supplementary Figure 27: (a) correlation between median moran's I and median residual from soil hot drought framework, (b) Amplitude augmented clustering model show higher regression than the null model indicating non-randomness a b

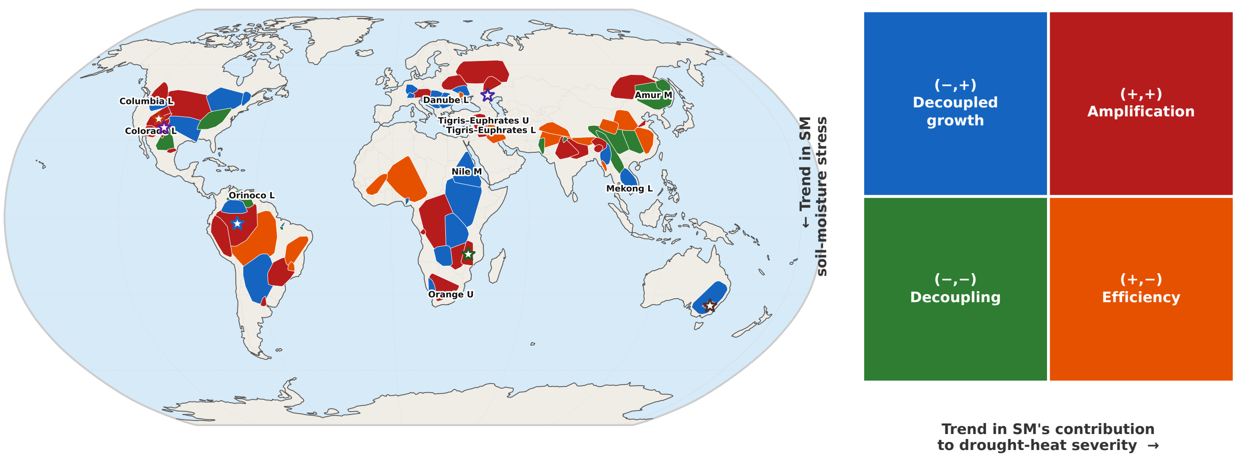

(+,+) — Amplification: Coherent drying amplify hot drought AND itself increasing

(+,−) — Efficiency: Coherent drying amplify hot drought AND itself decreasing

(−,+) — Decoupled — growth: Coherent drying does not amplify hot drought AND itself increasing

(−,−) — Decoupling: Coherent drying does not amplify hot drought AND itself increasing

Supplementary Figure 28: (a) Trend in coherent drying and trend in how much coherent drying explains hot drought severity (b) The bivariate key showing the colors corresponding to different categories

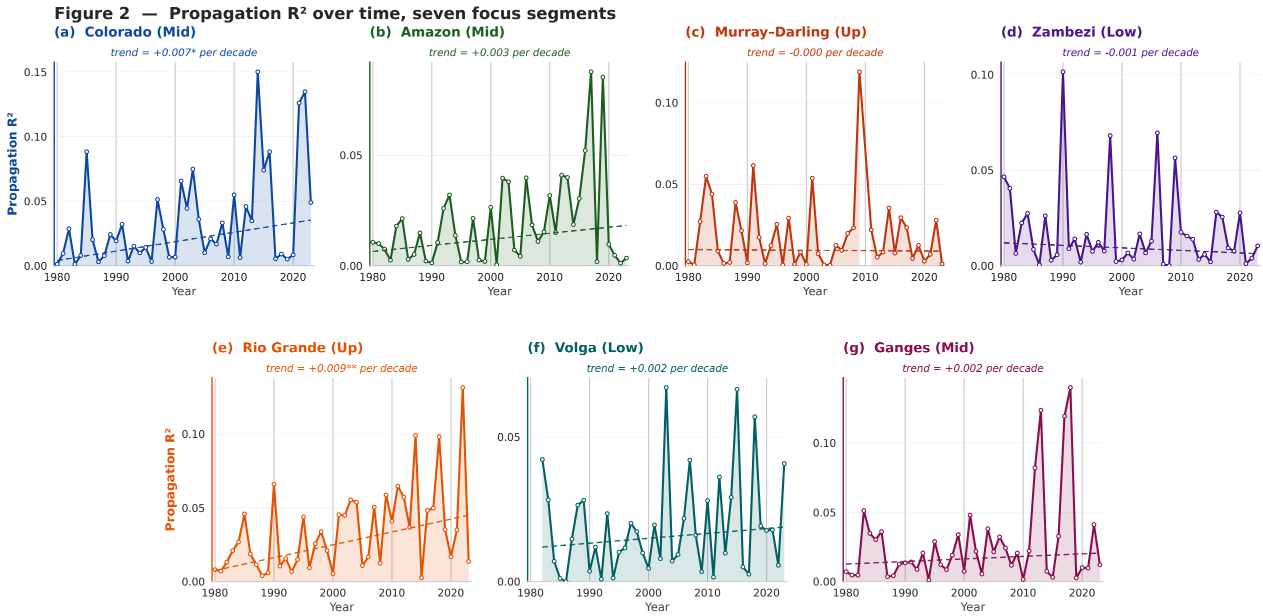

Supplementary Figure 29: Explainability of hot drought severity via remote proagation over(a) Colorado middle (b) Amazon middle, (c) Murray Darling upper, (d) Zambeji lower, (e) Rio grande upper, (f) Volga lower, (g) Ganges middle